JCI The Journal of Clinical Investigation

Neutrophils contribute to spontaneous resolution of liver inflammation and fibrosis via microRNA-223

Carolina Jimenez Calvente, … , Josh Boyer, Ariel E. Feldstein

J Clin Invest. 2019. https://doi.org/10.1172/JCI122258.

Research In-Press Preview Hepatology

Persistent, unresolved inflammation in the liver represents a key trigger for hepatic injury and fibrosis in various liver diseases and is controlled by classically activated pro-inflammatory macrophages, while restorative macrophages of the liver are capable of reversing inflammation once the injury trigger ceases. Here we have identified a novel role for neutrophils as key contributors to resolving the inflammatory response in the liver. Using two models of liver inflammatory resolution, we found that mice undergoing neutrophil depletion during the resolution phase exhibited unresolved hepatic inflammation, activation of the fibrogenic machinery and early fibrosis. These findings were associated with an impairment of the phenotypic switch of pro-inflammatory macrophages into a restorative stage after removal of the cause of injury and an increased NLRP3 / miR-223 ratio. Mice with a deletion of the granulocyte specific miR-223 gene showed a similarly impaired resolution profile that could be reversed by restoring miR-223 levels using a miR-223 3p mimic or infusing neutrophils from wildtype animals. Collectively, our findings reveal a novel role for neutrophils in the liver as resolving effector cells that induce pro-inflammatory macrophages into a restorative phenotype, potentially via miR-223.

Neutrophils contribute to spontaneous resolution of liver inflammation and fibrosis via microRNA-223

Carolina Jimenez Calvente[1]*, Masahiko Tameda[1]*, Casey D. Johnson[1], Hana del Pilar[1], Yun Chin Lin[1], Nektaria Adronikou[2], Xavier De Mollerat Du Jeu[2], Cristina Llorente[3], Josh Boyer[3], Ariel E. Feldstein[1]

[1]Department of Pediatrics, UCSD, USA;

[2] Thermofisher Scientific, Carlsbad; USA;

[3] Department of Medicine, UCSD, USA;

*These authors contributed equally to this work.

Conflict of interest: The authors declare that no conflict of interest exists.

Key words: Liver inflammation resolution, Neutrophils, microRNAs, liver fibrosis.

Corresponding author:

Dr. Ariel E. Feldstein

Professor of Pediatrics

Chief, Division of Pediatric Gastroenterology,

Hepatology, and Nutrition UCSD

3020 Children's Way, MC 5030

San Diego, CA 92103-8450

Tel: (858) 966-8907

Email: afeldstein@ucsd.edu

Abstract

Persistent, unresolved inflammation in the liver represents a key trigger for hepatic injury and fibrosis in various liver diseases and is controlled by classically activated pro-inflammatory macrophages, while restorative macrophages of the liver are capable of reversing inflammation once the injury trigger ceases. Here neutrophils as key contributors to resolving the inflammatory response in the liver. Using two models of liver inflammatory resolution, we found that mice undergoing neutrophil depletion during the resolution phase exhibited unresolved hepatic inflammation, activation of the fibrogenic machinery and early fibrosis. These findings were associated with an impairment of the phenotypic switch of pro-inflammatory macrophages into a restorative stage after removal of the cause of injury and an increased NLRP3 / miR-223 ratio. Mice with a deletion of the granulocyte specific miR-223 gene showed a similarly impaired resolution profile that could be reversed by restoring miR-223 levels using a miR-223 3p mimic or infusing neutrophils from wildtype animals. Collectively, our findings reveal hepatic neutrophils as resolving effector cells that induce pro-inflammatory macrophages into a restorative phenotype, potentially via miR-223.

Introduction

Liver inflammation constitutes a central contributor to liver pathology during chronic injury from varying etiologies (1,2). While it is self-limiting, liver inflammation is considered beneficial and contributes to tissue homeostasis (2). The inability to shut down the persistence of the triggers of the inflammatory response results in tissue dysfunction and perpetuates the disease state (3). Inflammation in the liver is typically characterized by *de novo* recruitment of a repertoire of inflammatory cells mainly composed of monocytes, early activated proinflammatory macrophages, neutrophils and NK cells that compromise hepatic vasculate architecture and function (4). The systemic response to persistent inflammation is impaired wound healing with subsequent activation of fibrogenic pathways and an overall progression to fibrosis – the excessive accumulation of extracellular matrix (ECM) (5) – that potentially leads to cirrhosis, which sets the stage for hepatic decompensation, primary liver cancer and death (6). In some instances, the liver can reverse injurious and fibrotic changes with the use of direct-acting antiviral agents directed to treat chronic hepatitis C virus (HCV) infection, corticoid therapy in patients with autoimmune hepatitis, cessation of alcohol consumption in patients with alcoholic liver disease (ALD) or bariatric surgery to induce significant and sustained weight loss in obese patients with nonalcoholic steatohepatitis (NASH) (7, 8, 9, 10, 11, 12). Therefore, it is of paramount importance to uncover the mechanism involved in the natural (also called spontaneous) resolution of liver inflammation in order to identify potential novel targets for therapeutic intervention in those patients that either do not respond to current therapies, or for whom no effective interventions are currently available.

Neutrophils have recently emerged as important contributors to the resolution of the inflammatory response in various tissues, including the heart, skin and joints (13, 14, 15, 16, 17). However, the mechanism by which neutrophils contribute to the resolution of inflammation remains incompletely understood.

MicroRNAs, naturally occurring small RNA molecules, play an important role in the regulation of gene expression involved in a variety of cellular processes, including inflammation. Several microRNAs have been identified as being involved in hepatic pathophysiology. Among them, miR-223, which is preferentially expressed in granulocytes (18, 19) and is a critical negative regulator of NLRP3 Inflammasome activity (18, 20), has been identified as one of the most significantly down regulated microRNAs in the livers of patients with NASH (21), while miR-223 knockout mice are highly sensitive to liver inflammation and injury when exposed to low dose endotoxin injection (19). In this study we examined the role of neutrophils during the resolution phase of liver inflammation and uncovered miR-223 as a novel anti-inflammatory, anti-fibrotic therapeutic target.

Results

Neutrophil depletion impairs spontaneous resolution of liver inflammation (SRLI). To study the role of neutrophils as potential mediators of SRLI, we first established a mouse model of systemic neutrophil depletion during the spontaneous recovery of liver inflammation after cessation of the cause of injury. The mice were gavaged for one week with carbon tetrachloride (CCL4) to induce liver inflammation. One group of mice was sacrificed 4 h post CCL4 treatment to serve as a putative inflammatory baseline control (named as 4 h-post CCL4 group). The rest of the mice were allowed to recover from inflammation naturally for 96 h following the full-course treatment (1 wk) with CCL4. An independent group of these mice was subjected to systemic neutrophil depletion using an i.v. injection of anti-Ly6G mAb (serving as the 96 h-post-CCL4 + Anti-Ly6G mAb group) or PBS (representing the 96 h-post-CCL4 untreated control) at 0.1 mg/mouse for three consecutive days and was sacrificed 24 h post final injection (end of the 96 h resolution stage) (Figure 1A). When compared to an independent group of mice injected with the neutrophil depletion isotype control IgG2b mAb following the same i.v. regimen described above, the treatment with anti-Ly6G mAb lead to almost complete neutralization of circulating neutrophils (Supplemental Figure 1A-B) and significantly increased the serum levels of the liver inflammation surrogate

alanine aminotransferase (ALT) during the 96 h-post CCL4 resolution phase (Figure 1B; versus non neutrophil depleted mice). The livers from mice not treated with anti-Ly6G mAb exhibited almost complete recovery with no evidence of necro-inflammation at 96 h post-CCL4 administration when compared to the livers of mice sacrificed 4 h after CCL4 treatment (Figure 1C-D); these results corroborate previously published data (22). Furthermore, the neutrophil-depleted livers from anti-Ly6G mAb injected mice, displayed significant necro-inflammatory changes (*Ishak histology* scoring, 23) when compared to mice that did not receive anti-Ly6G mAb, and similar to those sacrificed 4 h after CCL4 treatment (Figure 1C-D), indicating a worsening of the liver architecture. In addition to the aforementioned observation, we observed areas within the liver densely occupied by macrophages which stained positive for F4/80 (Figure 1E); similar F4/80 positive liver area also confirmed in a different experiment replicate under the same set of conditions but using a different clone the anti-Ly6G antibody (Supplementary Figure 2 and 3).

Similarly, the serum levels of the inflammatory cytokine IL12 sharply increased (versus untreated controls) (Figure 1F), whereas the specific anti-inflammatory cytokine IL10, a marker of restorative macrophages (24), dramatically decreased (Figure 1G), indicating an impaired systemic inflammatory condition.

To further assess the pro-inflammatory function of neutrophils in SRLI, we defined a liver macrophage phenotype profile of our experimental groups in Figure 1A by staining with Abs specific for either pro-inflammatory (Ly6C) or restorative (CD163 and CD14) macrophage markers (24, 25, 26, 27, 28, 29). The area stained for Ly6C was significantly expanded in neutrophil-depleted mice when observed in relation to those mice that did not undergo neutrophil depletion (Figure 2A-B). Conversely, the staining for CD163 and CD14 positive macrophages was significantly lower in mice given anti-Ly6G mAb when compared to their control animals not treated with Anti-Ly6G mAb (Figure 2C-D). To further support these data, we determined that treatment with anti-Ly6G mAb resulted in a pronounced upregulation of transcripts of the monocyte chemoattractant *Ccl4* and *Ccl2 (*30, 31) (Figure 2E-F), which

partly correlated to the hepatic levels of CCL2 and the CCL3 and CCL4 receptor CCR5 (Supplementary Figure 4 and 5).

Taken together, these results illustrate the contribution of neutrophils in SRLI.

*Neutrophil deletion results in the persistence of classically activated hepatic macrophages during SRLI***.** To better understand the mechanisms by which neutrophils participate in SRLI, hepatic macrophages were isolated from our experimental mice (Figure 1A) and confirmed by FACS using F4/80 expression as a selection target (Supplementary Figure 6A**;** gating strategy shown in Supplemental Figure 7). Next, we performed a gene expression analysis of *iNos,* the key enzyme of (classically activated) pro-inflammatory macrophages, and the restorative macrophage-specific markers *Arg1*, *Il10* and *Ager* (a scavenger receptor enriched in putative, anti-inflammatory macrophages; 32, 33, 34). The expression of *iNos* mRNA was dramatically downregulated in the hepatic macrophages of mice that were allowed to recover for four days compared to the control mice that presented a pronounced inflammation 4 h post-CCL4 (Supplementary Figure 6B). In contrast, the mice that were treated with anti-Ly6G mAb during the recovery phase showed robust expression of *iNos* mRNA compared to the untreated control mice at 96 h-post CCL4 (Supplementary Figure 6B). Moreover, the group of mice treated with anti-Ly6G mAb displayed significant downregulation of both *Arg1* and *Il10* when compared to the untreated group (Supplementary Figure 6C-D). Accordingly, *Ager* expression was significantly reduced in neutrophil-depleted mice compared to the non-depleted control group at 96 h post-CCL4 (Supplementary Figure 6E), which further supports the anti-inflammatory role of neutrophils in the liver.

These results suggest that neutrophils play a pivotal role as negative regulators of classical macrophage activation in SRLI.

Neutrophil abrogation worsens spontaneous resolution of early liver fibrosis. Persistent activation of macrophages as a result of hepatic inflammation typically initiates early fibrogenesis (5), a wound-healing response consisting of increased collagen production by activated hepatic stellate cells (HSCs) (5). We examined the potential effect of neutrophils

on downstream, persistent inflammation by performing Sirius Red and anti-αSMA staining in livers of mice from the experiment in Figure 1A to determine total collagen accumulation and HSCs activation, respectively. We observed negligible signs of collagen accumulation or HSC activation 96 h after the final scheduled dose of CCL4, as opposed to mice sacrificed 4 h after CCL4 treatment (Figure 3A-C), thus denoting fibrosis resolution. By contrast, the treatment with anti-Ly6G mAb to deplete neutrophils significantly exacerbated collagen deposition and enhanced HSC activation 96 h post-CCL4 administration when compared to mice untreated with anti-Ly6G mAb (Figure 3A-C); these results were replicated a different experiment repeat under the same condition but using other clone of the anti-Ly6G antibody (Supplementary Figure 2 and 3).

Likewise, the mRNA expression of the collagen degrading metalloproteinases, *Mmp3* and *Mmp8*, were significantly downregulated, especially *Mmp8*, in mice given anti-Ly6G mAb when compared to control mice that did not receive anti-Ly6G mAb (Figure 3D-E). By contrast, the transcript levels of the profibrotic gelatinase *Mmp9* after treatment with anti-Ly6G mAb showed an increasing tendency compared to IgG2B isotype control (Figure 3F). We also found transcript levels of *Timp1*, a positive regulator of fibrogenesis, to be substantially augmented in anti-Ly6G treated mice compared to control mice untreated with anti-Ly6G mAb (Figure 3G).

Neutrophils abrogation impaired spontaneous resolution of inflammation and advanced fibrosis in NASH. To elucidate the role of neutrophils beyond spontaneous resolution of toxin (CCL4)-induced inflammation and fibrosis, a dietary model of methionine and choline deficiency (MCD) that well resembles human fibrotic NASH was developed for six weeks and anti-Ly6G mAb-mediated neutrophil depletion (Supplementary Figure 8A-B) was conducted during a 2-week cessation period after the feeding course (spontaneous resolution period; Figure 4A). MCD-feed mice treated with IgG2B isotype and allowed to resolve spontaneously served as neutrophils depletion controls, while MCD-feed mice not allowed to resolve and given PBS represented the inflamed and fibrotic controls. Mice fed with methionine-supplemented diet (MCS) served as Wt controls. After two weeks of

cessation of the MCD feeding, depletion of neutrophils lead to a significant decrease of hepatic accumulation of anti-inflammatory macrophages (CD163 positive), as compared to IgG2B treatment control (Figure 4B,E). This was accompanied by a modest diminution of the abundance of total macrophages (F4/80 positive; Supplementary Figure 9A) and an increasing trend of the levels of *Tnfa, Il12* and *Nlrp3* transcripts (Supplementary Figure 9B-D), indicating a worsened inflammatory scenario.

Notably, treatment with anti-Ly6G mAb during cessation of MCD dieting further impaired the hepatic architecture, as shown by a significant increase of the activation of HSCs (αSMA positive) and a substantial accumulation of total collagen vs. treatment with IgG2b (Figure 4B, C-D), determining an impairment of fibrosis resolution.

Collectively, these results point towards a resolutive role of neutrophils during the cessation of injury dieting in NASH.

miR-223 loss of function worsens SRLI and early fibrosis. The granulocyte-specific microRNA, miR-223, has recently emerged as an endogenous post-transcriptional silencer of the pro-inflammatory sensor NlLRP3 through its 3' UTR (18, 20). To elucidate the underlying mechanism(s) by which neutrophils revert the activation of pro-inflammatory macrophages in the liver, miR-223 3p and *Nlrp3* were both measured by real time RT-PCR in hepatic macrophages isolated from our experimental mice in Figure 1. Neutrophil abrogation lead to a significant downregulation of hepatic macrophage miR223 3p levels compared to the expression of miR223 3p in hepatic macrophages of non-neutrophil depleted mice (Figure 5A). Consistent with these data, hepatic macrophages from neutrophil depleted mice showed a very significant upregulation of *Nlrp3* mRNA levels in hepatic macrophages versus miR-223 3p transcripts from the same mice (Figure 4A); this effect was not observed in the hepatic macrophages isolated from non-neutrophil depleted mice (Figure 5A).

CD177 is a surface membrane co-receptor specifically expressed in granulocytes (35, 36, 37, 38). It is principally involved in neutrophil migration (35) and it has been found to be

carried in extracellular vesicles (EVs), particularly microvesicles, released by neutrophils (38).

Because microvesicles are increasingly recognized as endogenous carriers of microRNAs (39) and macrophages and neutrophils are within close vicinity in the hepatic sinusoids (40, 41, 42, 43), we assessed the presence of CD177 in hepatic macrophages of Wt, miR-223-/- or anti-Ly6G mAb-treated mice during SRLI by staining with an anti-CD177 Ab to verify whether a neutrophil-mediated delivery could be the source of the miR-223 increase we found in hepatic macrophages of non-neutrophil depleted mice during SRLI (Figure 5A). The total number of anti-CD177 positive cells was higher in the hepatic macrophages from WT control mice when compared to those macrophages of anti-Ly6G mAb-treated, or miR-223-/- mice within the inflammation resolution period (Supplemental Figure 10A-B; Supplemental Figure. 11A). Importantly, no fluorescent signal was found in anti-CD177 stained or unstained hepatic macrophages from a separate group of untreated WT mice, confirming non-constitutive expression of CD177 or autofluorescence (under 488 UV filter) in hepatic macrophages under basal conditions (Supplemental Figure 11A-B). These results suggest the presence of CD177 in hepatic macrophages during the inflammation resolution period, and therefore pointing towards a potential miR-223 delivery to hepatic macrophages via neutrophilic EVs.

To evaluate the role of miR-223 as a potential mediator of SRLI, miR-223 deficient mice (representing the miR-223 -/- group) or their age and gender-matched littermates (corresponding to the Wt control group) were given a regimen of CCL4, via oral gavage, following the same regimen as in Figure 1A**,** but shortened to 4 days. After the last treatment with CCL4, Wt or miR-223 -/- mice were euthanized immediately after a-96 h recovery phase from the inflammatory effect of CCL4 (Figure 5B). A separate group of miR-223-/- mice was post-transcriptionally replaced with an intravenous injection containing 1 mg/kg of the synthetic miR-223 3p, 24 h and 72 h after the last CCL4 treatment; this group represented the miR-223 3p- treated miR-223-/- mice (Figure 5B). All mice were euthanized 24 h after the last injection (96 h post-CCL4, end of resolution phase) (Figure 5B). A significant

increase in serum ALT levels of miR-223 -/- mice (versus Wt controls) suggested an apparent anti-inflammatory function of miR-223 during the resolution phase (Figure 5C), which was further supported when the miR-223 3p-treated miR-223-/- group reverted ALT levels to within the normal range (vs. miR-223-/- mice) (Figure 5C). Compared to untreated Wt mice, histopathological examination of miR-223-/- mice, and their age and gender matched littermates, revealed massive leukocyte infiltration, hepatocyte ballooning and fibril septae formation, more prominently in miR-223-/- mice, 4 h post-CCL4 (Supplemental Figure 12) as assessed following the *Ishak* scoring system (23); this effect was absent and ameliorated in Wt and miR-223-/- mice, respectively, 96 h post-CCL4 administration (Figure 5D-E), which indicates favourable resolution of inflammation within a greater timeframe. Hepatic necroinflammation was resolved to a lesser extent in miR-223-/- mice (vs. Wt) 96 h post-CCL4 (Figure 5D-E), while the administration of miR-223 3p modestly reverted this pathology (Figure 5D-E). Consistently with these data, the area occupied by anti-F4/80 antibody in the liver of miR-223-/- mice was significantly augmented (vs. Wt controls), while the treatment with miR-223 3p restored it (Figure 5D,F). Confirming these data, the serum from miR-223-/- mice exhibited upregulation of IL12 cytokine when compared to Wt controls (Figure 5G), while mice treated with miR-223 3p displayed a modest decrease of serum IL12 (Figure 5G), indicating worsening systemic inflammation.

To further evaluate the ant-inflammatory role of miR-223 in the macrophage compartment during SRLI, hepatic sections of mice from experiment in Figure 5B were stained with Abs for Ly6C, CD163 or CD14. miR-223-/- mice exhibited an augmented positive area for Ly6C (versus Wt controls), while miR223-/- treated with miR-223 3p overcame this effect (Figure 6A,B) and displayed an expanded CD163 positive area (Figure 6A,C). Similarly, the stained area for CD14 was markedly reduced in miR-223-/- mice (vs. Wt controls) and notably increased in miR-223-/- mice treated with miR-223 3p (vs. miR-223-/-) (Figure 6A,D), further supporting the pivotal role of miR-223 during SRLI. Moreover, *Ccl2* and *Ccl4* mRNA expression levels were upregulated in miR-223-/- (vs. Wt controls) and downregulated in the miR-223 replaced miR-223-/- mice (vs. miR-223-/-; Figure 6E-F), suggesting an augmented

de novo infiltration of pro-inflammatory macrophages/monocytes when miR-223 is absent in the liver and abrogated when miR-223 is post-transcriptionally replaced with miR-223 3 p treatment.

Together, these results are in alignment with those found under neutropenia conditions during SRLI, suggesting that miR-223 might play a pivotal role in neutrophil-associated resolution of inflammation after cessation of an exogenous stressor.

To further uncover the link between neutrophils and the spontaneous resolution of early liver fibrosis, total collagen and HSC activation were assessed in liver sections of Wt control, miR-223-/- or miR-223 3p-treated miR-223-/- mice from the experiment in Figure 5B. The areas positive for Sirius Red or anti-αSMA within the liver parenchyma of miR-223-/- mice were significantly expanded when compared to WT control mice (Supplementary Figure 13A-C). By contrast, the liver architecture of miR-223-/- mice treated with miR-223 3p significantly improved in comparison to WT controls, as shown by an overall reduction in the area stained positive for Sirius Red or anti-αSMA antibody (Supplementary Figure 13A-C). Correlating these results, we found the expression of both *Mmp3* and *Mmp8* to be dramatically downregulated in miR-223-/- mice versus WT controls, and upregulated in miR-223-/- mice treated with miR-223 3p (vs. miR-223-/- mice; Supplementary Figure 13D-E); this indicates that collagen deposition is exacerbated by the absence of miR-223 during the spontaneous resolution phase of early liver fibrosis.

To confirm that endogenous, anti-inflammatory miR-223 has a neutrophilic source in liver during SRLI, neutrophils isolated from the peritoneal cavity of Wt (Wt neutrophils) or male, untreated, miR-223 deficient mice (miR-223-/y Neu) were infused intravenously to female miR-223-/- mice during resolution phase (96 h) after a-week course of CCL4 gavage (Figure 7A); CCL4-treated miR223-/- mice infused with miR-223-/y Neu represented the inflammation controls while those infused with PBS served as the neutrophil infusion control group. One day later, CCL4-treated miR-223-/- mice infused with Wt neutrophils significantly decreased collagen deposition, modestly reduced the populations of total macrophages ($F4/80^+$) and monocytes ($Ly6C^+$) and significantly increased the accumulation of anti-

inflammatory macrophages ($CD163^+$) in the liver parenchyma as compared to controls infused with untreated miR-223-/y Neu (Figure 7B-F).

Collectively, these results denote a novel contribution of neutrophils, via miR-223, in the spontaneous resolution of inflammation and liver injury after the causative insult has been ceased.

miR-223 deficiency hinders alternative activation of hepatic pro-inflammatory macrophages during SRLI. To uncover the cellular mechanism by which miR-223 participates in SRLI, total hepatic macrophages isolated from untreated miR-223-/-, or their Wt controls, were analysed by FACS to determine the percentage of total, pro-inflammatory and restorative macrophage populations (gating strategy shown in Supplemental Figure 14). The total hepatic macrophage population (CD11b positive cells) of miR-223-/- mice was predominantly composed of pro-inflammatory macrophages (double Ly6C and F4/80 positive cells) (Figure 8A-B), while restorative, alternatively activated, macrophages (double CD206 and F4/80 positive cells) were the dominant population in Wt controls (Figure 8A-B). These data were confirmed by a significant expansion of the pro-inflammatory hepatic macrophage population (double Ly6C and F4/80 positive cells) in miR-223-/- mice compared to the same population in the Wt control mice (Figure 8A-B). The levels of *iNos* mRNA were upregulated in the hepatic macrophages of miR-223-/- mice, while *Arg1* transcripts were notably decreased (Supplemental Figure 15). This effect was not observed in the hepatic macrophages taken from miR-223 3p-treated mice as these mice displayed an inversed mRNA expression pattern where *Arg1* was enhanced and *iNos* was decreased, when compared to miR-223-/- mice (Supplemental Figure 15).

These results indicate that miR-223 mediates alternative activation of hepatic pro-inflammatory macrophages during the SRLI.

miR-223 deletion exacerbates NLRP3 expression in hepatic macrophages during SRLI. To further elucidate the molecular mechanism that miR-223 utilizes to induce a restoring phenotype in hepatic macrophage during SRLI, isolated hepatic macrophages from Wt controls, miR-223-/- or miR-223 3p-treated miR-223-/- mice were subjected to gene

expression analysis of miR-223 3p and *Nlrp3 (*Figure 9A*)*. Hepatic macrophages of miR-223-/- mice exhibited notably higher expression of *Nlrp3* mRNA v.s. Wt controls, while those of miR-223-/- mice treated with miR-223 3p dramatically reduced this effect when compared to *miR-223*-/- mice (Figure 9A). Confirming these data, *Nlrp3* transcripts were abruptly augmented in hepatic macrophages of miR-223-/- mice relative to their own expression levels of miR-223 3p (Figure 9A). This effect was not observed in the hepatic macrophages from miR-223-/- mice supplemented with miR-223 3p, which displayed a very significant downregulation of *Nlrp3* mRNA vs. their miR-223 3p expression levels (Figure 9A). To further verify these results, we employed confocal microscopy to assess the expression pattern of NLRP3. The percentage of cells positive for NLRP3 was significantly increased in miR-223-/- mice when compared to the WT controls (Figure 9B-C; merges shown in Supplemental Figure 16). Conversely, the miR-223 3p-treated miR-223-/- mice exhibited a diminution of NLRP3 positive cells versus miR-223-/- mice (Figure 9B-C; merges shown in Supplemental Figure 16). These results further prove that miR-223 regulates NLRP3 post-transcriptionally during SRLI.

The p50 subunit of the transcription factor NF-kB has been attributed other functions beyond inflammation through the regulation of IL10 transcription (44, 45). To explore the upstream effect that miR-223-induced *Nlrp3* silencing might exert on hepatic macrophages during SRLI, the mRNA expression of *Nfkb* p50 and *Il10* were measured in hepatic macrophages from Wt, miR-223-/- or miR-223 3p-treated miR-223-/- mice. The levels of *Nfkb* p50 and *Il10* mRNA were robustly diminished in miR-223-/- mice when compared to their respective Wt control mice (Figure 9D-E). In contrast, the levels of *Nfkb* p50 *and Il10* transcripts in miR-223-/- mice treated with miR-223 3p were substantially increased vs. miR-223-/- mice (Figure 9D-E); these results suggest that the alternative activation of hepatic macrophages during SRLI might involve miR-223-mediated silencing of NLRP3 that in turns upregulates *Nfkb* p50 and subsequently *Il10*.

Conclusively, during spontaneous resolution of liver inflammation, our data collectively enlighten neutrophil derived miR223 as a silencer of *Nlrp3* in hepatic macrophages, which in

turn polarize to a restorative phenotype that reduces the release of IL10, thus mitigating fibrogenesis by impairing the activation of HSCs and collagen synthesis (Figure 10).

Discussion

Inflammation is a physiological response to tissue injury, or infection that leads to the secretion of various inflammatory mediators, such as cytokines, chemokines and eicosanoids that are responsible for coordinating the mechanisms of cellular defence and tissue repair (46). A persistent inflammatory state results in chronic adaptations that in turn exacerbate tissue injury and may result in an abnormal wound healing response contributing to the development of liver fibrosis (47). The natural, spontaneous resolution of inflammation is now recognized as a highly coordinated cellular event that is characterized by a phenotypic transition of pro-inflammatory macrophages into restorative macrophages under the control of endogenous pro-resolving mediators that enable the restoration of tissue homeostasis (48). Information regarding the molecular events that mediate the resolution of ongoing inflammation in the liver is limited to pro-resolving specialized mediators, a novel class of autacoids that act as “stop-signals” of the inflammatory response, including molecules such as n-3–derived resolvins, protectins, and maresins, as well as arachidonic acid–derived (n-6) lipoxins (49, 50, 51). Defective pro-resolving mechanisms may represent important novel contributors to persistent hepatic inflammation and suggest the possibility that abrogation of tissue inflammation could be achieved by exploiting active naturally occurring pro-resolving mechanisms instead of the classical passive blockade of pro-inflammatory mediators.

While neutrophils have been canonically viewed as the first wave of defence against infection and tissue damage (52), they have been increasingly recognized as novel resolving cells during the wound healing response in various tissues including the heart, skin and joints (13, 14, 15, 16, 17). In the liver, neutrophil infiltration is a key histopathological feature of chronic liver conditions such as NASH and ALD (53, 54).

In addition, the extent of neutrophil infiltration in the liver has been recently recognized as a key positive prognostic factor in patients with ALD (55). However, the role of neutrophils during the resolution phase of inflammation, and the underlying mechanisms of that process, have yet to be explored. In our current study, our findings uncover a novel regulatory role of neutrophils as contributors to the spontaneous resolution of liver inflammation (SRLI) and identified miR-223 as a potential key mediator of these effects.

Using a well-established murine model of SRLI, we found that systemic neutrophil depletion in these mice leads to a worsening in overall liver inflammation and impaired transition of hepatic pro-inflammatory macrophages into a restorative phenotype both in vivo and ex vivo, and results in changes to the chronic inflammatory and advanced fibrosis stage of the human resembled NASH model MCD dieting. These findings lead us to anticipate that a granulocyte-specific component must orchestrate the resolutive role that neutrophils acquire during SRLI.

MiR-223 is a granulocyte-specific, short, non-coding, double stranded RNA (18, 19) that has been identified as a post-transcriptional regulator of NLRP3 Inflammasome activity (18, 20) – a critical danger sensor protein that is activated during tissue injury and mounts a robust monocyte/macrophage-driven inflammatory response via maturation and secretion of the pro-inflammatory cytokines IL1β and IL18 (56). Interestingly, miR-223 knockout mice are highly sensitive to liver inflammation and injury when exposed to low-dose endotoxin injection (19). Moreover, untargeted hepatic microRNA profiling in patients with NASH has identified miR-223 as one of the top significantly down regulated microRNAs (21) compared to patients with fatty liver, or normal healthy control patients, and pro-inflammatory macrophages from adipose tissue have been shown to polarize to a restorative phenotype through the action of miR-223 in obesity-associated chronic inflammation (57). Our results demonstrate that the suppression of miR-223 expression recapitulated the effects on inflammation resolution that we found via the depletion of neutrophils, and denoted a negative regulatory role of miR-223 on *Nlrp3* mRNA expression in pro-inflammatory hepatic macrophages, therefore suggesting the mechanism by which miR-223 mediates their

alternative activation during SRLI. These data are consistent with previous published studies on extra-hepatic macrophages under resolutive conditions (13, 14, 15, 16, 17).

miR-223, as any other RNA, may be present within the extracellular compartment in two distinct forms: either encapsulated in EVs, or in a nonmembrane-bound form associated with specific proteins such as argonaute 2 (Ago2) and lipoproteins, which shield microRNAs from degradation (39). While naked or protein-bound microRNA cannot integrate into target cells due to its overall size and negative charges (39), EVs enable them to penetrate recipient target cells acting as a safe and efficient delivery vehicle (39). Recent evidence has shown that neutrophil-derived EVs contribute to inflammation resolution in models of joint inflammation driven by NLRP3 inflammasome activation, in part by suppressing the response to Toll-like Receptor (TLR) ligands in monocyte-derived macrophages and dendritic cells (15,16); Our data suggest that the transfer of miR-223 via EVs might represent a novel cell-to-cell communication platform between neutrophils and macrophages. The close proximity of macrophages and neutrophils within the sinusoidal space of the injured liver parenchyma possibly facilitates this interaction (40, 41, 42, 43) (Supplementary Figure 17). CD177 is a granulocyte-specific cell surface co-receptor that has been used as a specific marker of neutrophil-derived EVs (38). We observed the presence of CD177 in isolated hepatic macrophages of non-neutrophil depleted mice during SRLI, while CD177 was absent in hepatic macrophages of both miR-223-/- and neutrophil depleted mice during SRLI. These findings were associated with a reduced restorative hepatic macrophage compartment and an increase in the pro-inflammatory macrophage population in miR-223-/- mice, as well as the neutrophil-depleted mice, and a reduced inflammation and fibrosis after infusing neutrophils isolated from Wt mice to those undergoing SRLI in a miR-223-/- background, suggesting that neutrophils might induce a restorative phenotype in liver macrophages by delivering miR-223 within EVs.

The robust diminution in transcript expression levels of the anti-inflammatory cytokine *Il10*, and its transcription factor *Nfkb* p50, in hepatic macrophages of miR-223-/- mice carries the potential to be the upstream mechanism by which miR-223-derived *Nlrp3* silencing possibly

leads to an alternative activation of pro-inflammatory hepatic macrophages during SRLI without inducing changes in IL1β expression (data not shown). Importantly, serum levels of IL10 and the pro-inflammatory IL12 cytokine were down and up-regulated, respectively, in mice that underwent systemic neutrophil depletion. This suggests an extra-hepatic effect of neutrophils in the resolution of inflammation, which is consistent with previously published data (13, 14, 15, 16, 17).

The persistence of pro-inflammatory hepatic macrophages and liver inflammation that our data revealed in neutrophil-depleted, as well as miR-223-/- mice, culminated in changes to early fibrosis patterns with significant fibrogenic activity and increased collagen deposition in the livers of these mice, thus supporting the link between persistent inflammation and liver fibrosis development. Treatment of miR-223-/- mice with nanoparticle delivered-miR-223 3p restored inflammation resolution and protected against fibrosis. These results have significant translational implications for a variety of human hepatic, and potentially extra-hepatic disorders where NLRP3-mediated persistent inflammation may represent an important driver for injury and fibrosis development.

Our data, together with previous evidence associating hepatic neutrophil infiltration with a positive outcome of alcoholic hepatitis (55), point towards a distinct phenotype of neutrophils directly influenced by the stage of the inflammatory response: classic, pro-inflammatory neutrophils remain as key players of acute response but might acquire a pro-resolving phenotype when injury trigger ceases or persist but tolerance arises.

In conclusion, our findings uncover a novel role for neutrophils during the resolution phase of liver inflammation and identified miR-223 as a novel, potential anti-inflammatory and anti-fibrotic target.

Methods

Mice. Mouse studies were performed under permission and guidelines of the Institutional Animal Care and Use Committee (IACUC) of the UCSD. Eight-wk old female C57BL/6N and

male or female B6 Cd45.1 mice at 7 to 8 wks of age, were purchased from Jackson Laboratories (Sacramento, CA). Eight-wk old female or male miR-223-/- mice purchased from Jackson Laboratories in a B6 Cd45.1 background, were allowed to breed at 25 °C housing with 12-hour light/dark cycle; the allelic composition of these mice was Mir223^{tm1Fcam} and their background involved 129S4/SvJae and C57BL/6 mice.

SRLI post-CCL4 intoxication. To induce liver inflammation, CCL4 diluted in mineral oil (m.o.) was given once to 8-wk old female C57BL/6 mice by oral gavage at 0.875 ml/kg. Three days later, the CCL4 dose was increased to 1.75 ml/kg and was given every 3 days up to one week. Mice gavaged with m.o. served as non-inflamed wild type (Wt) controls. A group of mice was euthanized 4 h after CCL4 gavage to serve as inflamed controls, and two other groups were allowed to recover inflammation for 4 days and euthanized immediately after.

SRLI in 7 to 8-wk old female or male miR-223-/- mice and their age and gender matched littermate controls (in a B6 Cd45.1 background) was induced as above but shortening CCL4 regimen to 4 days instead of 9, to avoid death particularly observed in these knock out mice.

Systemic neutrophil depletion in SRLI. To deplete neutrophils systemically during SRLI, the above C57BL/6 mice that were allowed to recover inflammation after CCL4 treatment, were given one i.v. injection of PBS or monoclonal anti-Ly6G antibody (clone RB6-8C5; Cat number 14-5931-82, ThermoFisher Scientific, Carlsbad, CA) at 0.1 mg/mouse from day 1 to 3 of the recovery period. One day later, the mice were euthanized. Mice injected with PBS served as inflammation recovery controls, while mice injected with rat IgG2b isotype control (Cat number 40064, BioLegend, 3 San Diego, CA) served as negative controls of neutrophil depletion.

Neutrophil depletion in the SRLI-post CCL4 model replicated for the revision of this paper, was performed with the clone 1A8 of the anti-Ly6G mAb (Cat number 127649 BioLegend).

SRLI post-MCD dieting. Eight-wk old male C57BL/6N mice were fed *ad libitum* for one wk and immediately after, the feeding was changed to a methionine and choline deficient (MCD diet; A02082002B, Research Diets, Inc., New Brunswick, NJ) or supplemented (MCS control diet; A02082003B, Research Diets, Inc.) diet to induce fibrotic NASH. Six weeks later, mice

were immediately euthanized to serve as MCD positive or MCS negative inflammation controls, and two independent groups fed with MCD were dieted with control MCS for two weeks to allow SRLI. Then, anti-Ly6G mAb (clone RB6-8C5; Thermofisher Scientific) or rat IgG2b isotype (Biolegend) was given intraperitoneally at 200 µg/ mouse every four days during the two-wk SRLI period; mice injected with IgG2b isotype represented the neutrophil depletion control. Twenty-four hours after the last injection, mice were sacrificed to harvest the liver, collect blood and assess inflammation and fibrosis in liver biopsies.

miR-223 post-transcriptional replacement. An independent group of miR-223-/- mice treated with CCL4 and allowed to spontaneously recover inflammation for 96 h as described above, were intravenously injected with *miR-223* 3p at 1 mg/kg 24 h and 72 h after last CCL4 treatment. A mimic of miR-223 was encapsulated as *in vivo* ready *mirVana* mmu-miR-223 3p (mature sequence UGUCAGUUUGUCAAAUACCCCA) in *Invivofectamine3*® (Thermo Fisher Scientific, Carlsbad, CA) according to manufacture´s instructions, to allow safe systemic delivery.

*Neutrophil isolation and infusion***.** Neutrophils were isolated from male C57BL/6N mice or male miR-223$^{-/y}$ mice using a neutrophils (mouse) isolation kit (Cayman chemical, Ann Arbor, MI) according to manufacture's instruction. Female miR-223$^{-/-}$ mice treated for a-week course of CCL4 were injected once with 5 x 10^6 isolated neutrophils via intravenous injection at day 1 of the recovery period (4 days post-CCL4 treatment). Three days after neutrophil injection, the mice were euthanized to harvest liver tissue.

*Histology and IHC***.** 4 µm thick formalin fixed liver sections were preincubated with 3% hydrogen peroxide for 10 min and blocked with 5% BSA at RT for 2 h. Primary rat monoclonal anti-Ly6C (1:100 dilution; Cat number ab15627, Abcam, Cambridge, United Kingdom) or anti-F4/80 (1:50; Cat number MCA497GA, Biorad, Hercules, CA) and rabbit monoclonal anti-CD163 (1:500; Cat number ab182422, Abcam) or polyclonal anti-CCR5 (1:100; Cat number PA5-78949, Invitrogen), αSMA (1:500; Cat number ab124964, Abcam) or polyclonal anti-CD14 (1:100; Cat number sc-9150, Santa Cruz Biotechnologies) Abs were

incubated on the blocked sections at 4°C in Dako (Odense, Denmark) Antibody Diluent with Background Reducing Components, except anti-Ly6C Ab that was diluted in PBS containing 1% BSA + 1% FBS. With the exception of anti-F4/80 Ab that required antigen retrieval in TBS-T with 2% BSA + 1% triton x-100 for 30 min at RT, the rest of Abs were antigen retrieved in boiling citrate buffer (except for anti-CCR5 antibody; pH 9) for 20 min. Permeabilization with 0.2% tween-20 in PBS for 30 min was required before the blocking step in the sections to be incubated with anti-Ly6C Ab. After overnight incubation with primary Ab, the sections were washed in TBS-tween and incubated with ready to use HRP-linked anti-rat or rabbit secondary IgG Ab (Immpress HRP reagents, Vector Labs, Burlingame, CA) for 1 h at RT. Color was developed with DAB solution (Vector Labs) for up to 10 seconds. Nuclei were then counterstained with Mayer's hematoxylin (Sigma-Aldrich, St. Louis, MO) for 2 min, followed by dehydration and embedding in glycerol. F4/80, Ly6C, CD163, CD14 or αSMA positive cells were quantified in 10 randomly selected fields (x200 magnification) imaged using a Nanozoomer 2.0HT Slide Scanner microscope (Hamamatsu Photonics K.K., Hamamatsu, Japan). The area occupied was analyzed by selecting brown areas using an unchanged threshold value in macro function of Image J software (NIH). Results were represented as percentage of area occupied by positive cells per total area in each specimen.

To identify collagen accumulation in liver tissue, formalin fixed hepatic sections of 4 μm thickness were stained for 2 h at RT with an aqueous solution of saturated picric acid (Sigma-Aldrich) mixed with 0.1% Fast Green FCF and 0.1% Direct Red Dye (Sigma-Aldrich). Ten randomly selected fields (x100 magnification) were imaged and photographed as above, and the percentage of Sirius red-stained area was measured by Image J software with adjusted, unchanged threshold setting using macro function. Results were expressed as percentage of area occupied by Sirius red stained fibrils.

Immunofluorescence in primary hepatic macrophages. $75x10^3$ cells were plated overnight on a Nunc Lab-Tek II 4-well chamber slide (Thermo Fisher, Carlsbad, CA) to allow attachment

and differentiation. After 18-20 h incubation at 37°C, 5% C02 and 85-98% humidity, the cells were washed and fixed with 4% paraformaldehyde for 10 min at RT. Next, the cells were washed, permeabilized (0.2% tween 20 in PBS 30 min), and incubated at 4°C with mouse monoclonal anti-NLRP3 (1:100; Cat number AG-20B-0014-C100, AdipoGen, San Diego, CA) or rabbit polyclonal anti-CD177 (1:50; Cat number ab203025, Abcam) antibody diluted in Dako Ab Diluent with Backgorund Reducing Components. After overnight incubation, the cells were washed and treated with Alexa Fluor 488 anti-rabbit or Alexa Fluor 598 anti-mouse IgG Ab (1:1000; Invitrogen, Carlsbad, CA) for 1 h at RT on dark, followed by washing and 5 min nuclei staining with DAPI diluted at 1:200 in PBS. Chamber was then removed, and the cells were mounted on a cover glass with Dako Fluorescent Mounting Media and analysed with an Olympus FV1000 Confocal Microscope (Shinjuku, Tokyo, Japan) by repeat x-y scanning at 12.5 resolution pixels and unchanged laser power. Results are expressed as percentage of anti-NLRP3 positive cells or as a ratio of anti-CD177 positive areas per total number of cells per field, analysed by macro function of Image J and normalized by total number of nuclear cells in each field (x450 magnification).

Serum ALT, and cytokines measurements. Mouse serum collected from 2 h-coagulated blood at RT, was subjected to alanine aminotransferase (ALT) analysis according to manufacturer's instruction (InfinityTM ALT, Thermo Fisher Scientific).

Serum IL12. Mouse IL12 was measured in 13 µl of diluted serum (1:5) with biotin-conjugate anti-mouse IL12 mAb, following the manufacturer's instruction (Mouse IL12 ELISA kit; Invitrogen).

Serum IL10. Mouse IL10 was quantified in 13 µl diluted serum (1:4) according to manufacturer's instruction (Mouse IL10 ELISA kit; Invitrogen), except TMB substrate addition that was replaced by chemiluminescent SuperSignal ELISA Femto (1:1 dilution; Thermo Fisher Scientific) incubation from 1 to 5 min on dark. Results were calculated from luminescence units in linear regression standard curve.

Blood neutrophil counting. Mouse blood smears collected from tail vain on glass slides, were allowed to dry briefly, and immediately fixed in pure methanol (Sigma-Aldrich) at RT. After 30 sec fixation, the smears were washed gently with tap water, dry overnight, and stained with 1:11 diluted Giemsa (Ricca Chemical, Arllington, TX) in Giemsa buffer (Sigma-Aldrich) for 45 min at RT.

Real time RT-PCR. Total RNA was isolated with TRIzol Reagent (Sigma-Aldrich). 1 µg of total RNA was reverse transcribed into cDNA using the iScript cDNA Synthesis Kit (BioRad, Hercules, CA). The following mouse SYBR green primers were purchased from Integrated DNA Technologies (ITD, Skokie, IL): *Ager* forward 5' TCACAGAAACCGGCGATGA 3', reverse 5' CGATCTGGGTGCTCTTACGG 3'; *Arg1* forward 5' CTCCAAGCCAAAGTCCTTAGAG 3', reverse 5' AGGAGCTGTCATTAGGGACATC 3'; *B2m* forward CCCCACTGAGACTGATACATA CG , reverse CGATCCCAGTAGACGGTCTTG; *Ccl2* forward 5' TTAAAAACCTGGATCGGAACCAA 3', reverse 5' GCATTAGCTTCAGATTTACGGGT 3'; *Ccl4* forward 5' TTCCTGCTGTTTCTCTTACACC 3'; reverse 5' CTGTCTGCCTCTTTTGGTCAG 3'; *Il10* forward 5' GCTCTTACTGACTGGCATGAG 3', reverse 5' CGCAGCTCTAGGAGCATGTG 3'; *Il12* p35 forward 5' GAGGACTTGAAGATGTACCAG 3', reverse 5' TTCTATCTGTGTGAGGAGGGC 3'; *iNos* forward 5' CAGCTGGGCTGTACAAACCTT 3', reverse 5' CATTGGAAGTGAAGCGGTTCG 3'; *Mmp3* forward 5' ACATGGAGACTTTGTCCCTTTTG 3', reverse 5' TTGGCTGAGTGGTAGAGTCCC 3'; *Mmp8* forward 5' CCTTGCCCATGCCTTTCAAC 3', reverse 5' TCATGAGCAGCCACGAGAAA 3'; *Nfkb* p50 forward 5' GGTCACCCATGGCACCATAA 3', reverse 5' AGCTGCAGAGCCTTCTCAAG 3'; *Nlrp3* forward 5' ATTACCCGCCCGAGAAAGG 3', reverse 5' TCGCAGCAAAGATCCACACAG 3'.

B2m was used to normalize data and to control for RNA integrity. cDNA amplification reactions were performed using a CFX96 real-time system (Bio-Rad, Hercules, CA).

Specific cDNA from miR-223 3p or U6, were transcribed from 10 ng total RNA by reverse transcriptase (RT) reaction with the TaqMan MicroRNA Reverse Transcription kit (Applied

Biosystems, Foster City, CA). TaqMan MicroRNA Assay kit specific for mmu-miR-223 3p and mmu-*U6* were employed for amplification reactions (Applied Biosystems). *U6* served as housekeeping gene. Reactions were performed in a Step One Plus real-time amplification system (Applied Biosystems).

TaqMan and SYBR green reaction mixtures were purchased from Applied Biosystems.

Gene expression data was calculated by the Delta Delta CT.

Isolation of liver macrophages. Multiple mouse livers were separately digested *in situ* by perfusing through the infra hepatic vein cave (IVC) with EGTA, pronase and collagenase D solutions subsequently as described (58). Then, each liver was placed individually in ice-cooled enzyme buffer solution (prepared as described (58) on ice and transferred to room temperature 30 min immediately before *in vitro* digestion with pronase and collagenase D solution (containing 1% DNAse) on a stirring plate for 24 min at 40°C as described elsewhere (58). Next, debris filtration and total liver cells precipitation, was performed as described (58). Parenchymal and non-parenchymal cells were gradient separated in two layers with 37.5% Nycodenz solution (Axis-Shield, Oslo, Norway) as previously shown (58). The non-parenchymal cell fraction was collected from the upper layer after centrifugation at 580*g for* 10 min at 4°C. The collected cell layer was then resuspended in MACS buffer (PBS with 2mM EDTA and 2% FBS) and incubated with rat, biotinylated F4/80 monoclonal antibody (1:100; Cat number 123105 BioLegend, San Diego, CA) at 1.25 g per 10^6 cells for 30 min on ice. Afterwards, the cells were washed in MACS buffer, centrifuged at 700*g* for 5 min at RT, resuspended in MACS buffer and incubated with 9 μl of anti-biotin micro beads (Miltenyi, Bergisch Gladbach, Germany) per 10^6 cells for 1 h at 4 °C on dark. Final macrophage collection was achieved with MACS magnetic cell separation columns (Miltenyi) according to manufacturer's instructions. For immunofluorescence and qRT-PCR analysis, the purity of the final isolated macrophages was enhanced by plating the cells on a T25 tissue culture flask with the macrophage/monocyte specific culture media RPM1-1640 (Gibco, Carlsbad, CA) containing 10% FBS and 1% antibiotic/antimicotic to get readout of possible unwanted non-parenchymal cells (stellate and endothelial cells). Cells were allowed

to attach and differentiate on plastic surface overnight in an incubator at 37°C, 5% C02 and 85-98% humidity.

About 1 to 4x10^6 macrophages were isolated per liver by this method.

*FACS analysis***.** Total liver macrophages resuspended in MACS buffer were fixed in 2% paraformaldehyde for 10 min at RT. After overnight storage at 4°C, the cells were washed, centrifuged and blocked with rat anti-CD16/32 mAb (1:500; Cat number 14-0161-82, Thermo Fisher) at RT for 15 min. Staining of total macrophages was then proceeded with 2 g of APC-anti-biotin streptavidin (Biolegend) at 4°C on dark. After 20 min, rat FITC-anti-CD11B (1:400; Cat number 101205, Biolegend), rat Brilliant Violet- 421-anti-Ly6C (2.5 µl per 0.5x10^6 cells; Cat number, 128031, Biolegend) and rat PerCP-Cy5.5-anti-CD206 (1:100; Cat number 141715 Biolegend) mAbs were incubated with the cells for 30 min at 4°C on dark. The cells were finally centrifuged, washed and resuspended in MACS buffer. Subsets of total macrophages were then identified with a FACSCanto RUO-ORANGE analyser (BD Bioscience, San Diego, CA) and represented as percentage of double positive F4/80 and Ly6C or CD206 cells at unchanged x,y values.

Immunoblot analysis Twenty of total tissue protein were loaded in 5% β-2-mercaptoethanol-contained SDS, boiled for 5 min and electrophoresed via an Any kD precast Tris-Glycine gel (Bio-Rad) at 60 v for 15 min, followed by 100 v until the end of the run. Tris-Glycine-SDS at pH 8.3 was used as a running buffer. After electrophoresis, the proteins were transferred from the gel to a nitrocellulose membrane in a Trans Blot Turbo Transfer® system (Bio-Rad) for 7 min at 25 v. An ethanol-based solution was used as transfer buffer (Bio-Rad). Once proteins were transferred, blocking of the membrane was proceeded for 1 h in TBS-tween-diluted 5% dried milk. The membrane was then incubated with mouse anti-CCL2 (1:000; Cat number 2029 Cell Signalling). After overnight incubation with primary antibody, the membrane was washed three times in TBS-tween and incubated with HRP-linked anti-mouse antibodies for 1h at RT. Finally, protein bands were visualized with an enhanced chemiluminescence reagent (Pico® or Femto; Thermo Fisher Scientific) and digitized in a CCD camera (ChemiDoc®, Bio-Rad). Intensity of bands were quantified

with Image J. Results are expressed as arbitrary units of protein expression normalized against the housekeeping protein ACTB housekeeping protein.

*Statistics***.** Shapiro Wilk test (alpha=0.05) was used to check normal Gaussian distribution (Supplementary Figure 18). Significances of two group comparisons were determined with two-tailed Student´s t-test. Significances of more than two groups were anallysed by one-way ANOVA. Significances of multiple comparisons between two or more groups were measured with two-way ANOVA. Tukey´s post hoc test was used to correct both one- and two-way ANOVA. *P*-values of <0.05 were considered significant. Error bars are represented as means ± SD. Experiments were repeated at least two or three times and assays were performed in duplicates or triplicates.

Study approval. The experimental protocols were approved by the IACUC of the UCSD under protocol S11200.

Acknowledgements

These studies were supported by the NIH (R01 DK113592 and U01 AA024206 to AEF), the microscopy core facility of the Department of Neuroscience at the UCSD (grant NS047101) and the Flow Cytometry Core at the San Diego Core Center for AIDS Research (P30 AI036214), the VA San Diego Health Care System, and the San Diego Veterans Medical Research Foundation.

Author contributions

CJC, partially conceived the idea, designed and performed experiments, analysed data and wrote the manuscript; MT designed and performed experiments and analysed data; CD, HDP, YCL, CLL and JB provided technical help; NA and XDMDJ supplied the miR-223 3p and Invivofectamin3®; AEF conceived the idea, helped design the experiments, provided the funding for the study, and helped draft and critically revised the manuscript**.**

Supplementary Information accompanies this paper online

References

1. Sun B, Karin M. Obesity, inflammation, and liver cancer. *J Hepatol*. 2012;56(3):704–713.

2. Robinson MW, Harmon C, O'Farrelly C. Liver immunology and its role in inflammation and homeostasis. *Cell Mol Immunol*. 2016;13(3):267-76.

3. Medzhitov R. Origin and physiological roles of inflammation. *Nature*. 2008;454(7203):428–435

4. Liaskou E, Wilson DV, Oo YH. Innate immune cells in liver inflammation. *Mediators Inflamm*. 2012;2012:949157.

5. Koyama Y, Brenner DA. Liver inflammation and fibrosis. *J Clin Invest*. 2017;5(1):55–64

6. Czaja AJ. Hepatic inflammation and progressive liver fibrosis in chronic liver disease. *World J Gastroenterol*, 2014;20(10):2515–2532.

7. Arthur MJP. Reversibility of liver fibrosis and cirrhosis following treatment for hepatitis C. *Gastroenterology*. 2002;122(5):1525–1528.

8. Czaja AJ, Carpenter HA. Decreased fibrosis during corticosteroid therapy of autoimmune hepatitis. *J Hepatol*. 2004;40(4):646–652

9. Dufour JF, DeLellis R, Kaplan MM. Reversibility of hepatic fibrosis in autoimmune hepatitis. *Ann Intern Med*. 1997;127(11):981–985

10. Lassailly G, et al. Bariatric surgery reduces features of nonalcoholic steatohepatitis in morbidly obese patients. *Gastroenterology*. 2015;149(2):379–388

11. Dixon JB, Bhathal PS, Hughes NR, O'Brien PE. Nonalcoholic fatty liver disease: Improvement in liver histological analysis with weight loss. *Hepatology.* 2004;39:1647–54

12. Ellis EL, Mann DA. Clinical evidence for the regression of liver fibrosis. *J Hepatol.* 2012;56(5),1171-80

13. Horckmans M, et al. Neutrophils orchestrate post-myocardial infarction healing by polarizing macrophages towards a reparative phenotype. *Eur Heart J*. 2017;38(3):187–197

14. Nishio N, Okawa Y, Sakurai H, Isobe KI. Neutrophil depletion delays wound repair in aged mice. *Age*. 2008;30(1),11–19

15. Cumpelik A, Ankli B, Zecher D, Schifferli JA. Neutrophil microvesicles resolve gout by inhibiting C5a-mediated priming of the inflammasome. *Ann Rheum Dis*. 2016; 75(6):1236–1245

16. Headland SE, et al. Neutrophil-derived microvesicles enter cartilage and protect the joint in inflammatory arthritis. *Sci Transl Med*. 2015;7(315):315

17. Kubes P. The enigmatic neutrophil: what we do not know. *Cell Tissue Res*. 2018;371(3):399-406

18. Bauernfeind F, et al. NLRP3 inflammasome activity is negatively controlled by miR-223. *J Immunol*. 2012;189(8):4175–4181

19. Johnnidis JB, et al. Regulation of progenitor cell proliferation and granulocyte function by microRNA-223. *Nature*. 2008;451:1125–1129

20. Neudecker V, et al. Myeloid-derived miR-223 regulates intestinal inflammation via repression of the NLRP3 inflammasome. *J Exp Med*. 2017;214:1737–1752

21. Cheung O, et al. Nonalcoholic steatohepatitis is associated with altered hepatic MicroRNA expression. *Hepatology*. 2008; 48(6):1810–1820

22. Ramachandran P, et al. Differential Ly-6C expression identifies the recruited macrophage phenotype, which orchestrates the regression of murine liver fibrosis. *Proc Natl Acad Sci*. 2012;109(46):E3186-95

23. Ishak K, et al. Histological grading and staging of chronic hepatitis. *J Hepatol*. 1995;22:696–699.

24. Jablonski KA, et al. Novel markers to delineate murine M1 and M2 macrophages. *PLoS ONE*. 2015;10(12):e0145342.

25. Bouhlel MA, et al. PPARγ Activation Primes Human Monocytes into Alternative M2 Macrophages with Anti-inflammatory Properties. *Cell Metabolism*. 2007;6(2):137–143

26. Sierra-Filardi E, Vega MA., Sánchez-Mateos P, Corbí AL, Puig-Kröger A. Heme Oxygenase-1 expression in M-CSF-polarized M2 macrophages contributes to LPS-induced IL-10 release. *Immunobiology*. 2010;215(9-10):788–795

27. Liu C, et al. Targeting the Shift from M1 to M2 Macrophages in Experimental Autoimmune Encephalomyelitis Mice Treated with Fasudil. *PLoS ONE*. 2013;8(2)**,** e54841

28. Sanyal R, et al. MS4A4A: a novel cell surface marker for M2 macrophages and plasma cells. *Immunol Cell Biol*. 2017;7:611-619

29. Martinez FO, Gordon S, Locati M, Mantovani A. Transcriptional Profiling of the Human Monocyte-to-Macrophage Differentiation and Polarization: New Molecules and Patterns of Gene Expression. *J Immunol*. 2006;177:7303–7311

30. Deshmane SL, Kremlev S, Amini S, Sawaya BE. Monocyte Chemoattractant Protein-1 (MCP-1): An Overview. *J Interferon Cytokine Res*. 2009;29(6):313–326.

31. Mantovani A, et al. The chemokine system in diverse forms of macrophage activation and polarization. *Trends Immunol.* 2004*;25(*12):677-86

32. Sica A, Mantovani A. Macrophage plasticity and polarization: In vivo veritas. *J Clin Invest.* 2012*;*122(3):787–795

33. Gordon S, Martinez FO. Alternative Activation of Macrophages: Mechanism and Functions. *Immunity*. 2010;32(5),593-604

34. Lolmede K, et al. Inflammatory and alternatively activated human macrophages attract vessel-associated stem cells, relying on separate HMGB1- and MMP-9-dependent pathways. *J Leukoc Biol*. 2009;85(5):779–787.

35. Sachs UJH, et al. The neutrophil-specific antigen CD177 is a counter-receptor for platelet endothelial cell adhesion molecule-1 (CD31). *J Biol Chem*. 2007;282(32):23603–23612.

36. Kissel K, Santoso S, Hofmann C, Stroncek D, Bux J. Molecular basis of the neutrophil glycoprotein NB1 (CD177) involved in the pathogenesis of immune neutropenias and transfusion reactions. *Eur J Immunol*. 2001;31(5),1301–1309

37. Bauer S, et al. Proteinase 3 and CD177 are expressed on the plasma membrane of the same subset of neutrophils. *J Leukoc Biol*. 2007;81(2):458–464

38. Timár CI, et al. Antibacterial effect of microvesicles released from human neutrophilic granulocytes. *Blood*. 2013;121(3):510–518

39. Arrese M, Eguchi A, Feldstein, AE. Circulating microRNAs: Emerging biomarkers of liver disease. *Semin Liver Dis*. 2015;35(1):43–54

40. Freitas-Lopes M, Mafra K, David B, Carvalho-Gontijo R, Menezes G. Differential Location and Distribution of Hepatic Immune Cells. *Cells*. 2017(4);6,48

41. Gong JP, et al. Liver sinusoidal endothelial cell injury by neutrophils in rats with acute obstructive cholangitis. *World J Gastroenterol*. 2002;8(2):342–345

42. Krenkel O, Tacke F. Liver macrophages in tissue homeostasis and disease. *Nat Rev Immunol*. 2017;17(5):306-321

43. Racanelli V, Rehermann B. The liver as an immunological organ. *Hepatology*. 2006;43(S1):S54-62

44. Wessells J, et al. BCL-3 and NF-kappaB p50 attenuate lipopolysaccharide-induced inflammatory responses in macrophages. *J Biol Chem*. 2004;279(48):49995–50003

45. Cao S, Zhang X, Edwards JP, Mosser DM. NF-KB1 (p50) homodimers differentially regulate pro- and anti-inflammatory cytokines in macrophages. *J Biol Chem*. 2006;281(36): 26041–26050

46. Weiss U. Inflammation. *Nature*. 2008;454:427

47. Wynn TA, Ramalingam TR. Mechanisms of fibrosis: Therapeutic translation for fibrotic disease. *Nat Med*. 2012;18:1028-40

48. Wynn TA, Vannella KM. Macrophages in Tissue Repair, Regeneration, and Fibrosis. *Immunity*. 2016;44(3):450-462

49. Kohli P, Levy BD. Resolvins and protectins: Mediating solutions to inflammation. *Br J Pharmacol*. 2009;158(4):960–971

50. Serhan CN, Yacoubian S, Yang R. Anti-Inflammatory and Proresolving Lipid Mediators. *Annu Rev Pathol*. 2008;3:279–312

51. Serhan CN, et al. Maresins: novel macrophage mediators with potent antiinflammatory and proresolving actions. *J Exp Med*. 2009;206(1):15–23

52. Uhl B, et al. Aged neutrophils contribute to the first line of defense in the acute inflammatory response. *Blood*. 2016;128(19):2327–2337

53. Brunt E. Histological assessment of nonalcoholic fatty liver disease in adults and children. *Clinical Liver Disease*. 2012;1(4):108–111

54. Theise ND. Histopathology of alcoholic liver disease. *Clinical Liver Disease*. 2013;2:64–67

55. Altamirano J, et al. A histologic scoring system for prognosis of patients with alcoholic hepatitis. *Gastroenterology*. 2014;146(5):1231–1239

56. Latz E, Xiao TS, Stutz A. Activation and regulation of the inflammasomes. *Nat Rev Immunol.* 2013;13(6):397-411

57. Zhuang G, et al. A novel regulator of macrophage activation: miR-223 in obesity-associated adipose tissue inflammation. *Circulation*. 2012;125(23),2892-903

58. Mederacke I, Dapito DH, Affò S, Uchinami H, Schwabe FR. High-yield and high-purity isolation of hepatic stellate cells from normal and fibrotic mouse livers. *Nat Protoc*. 2015;10:305–315

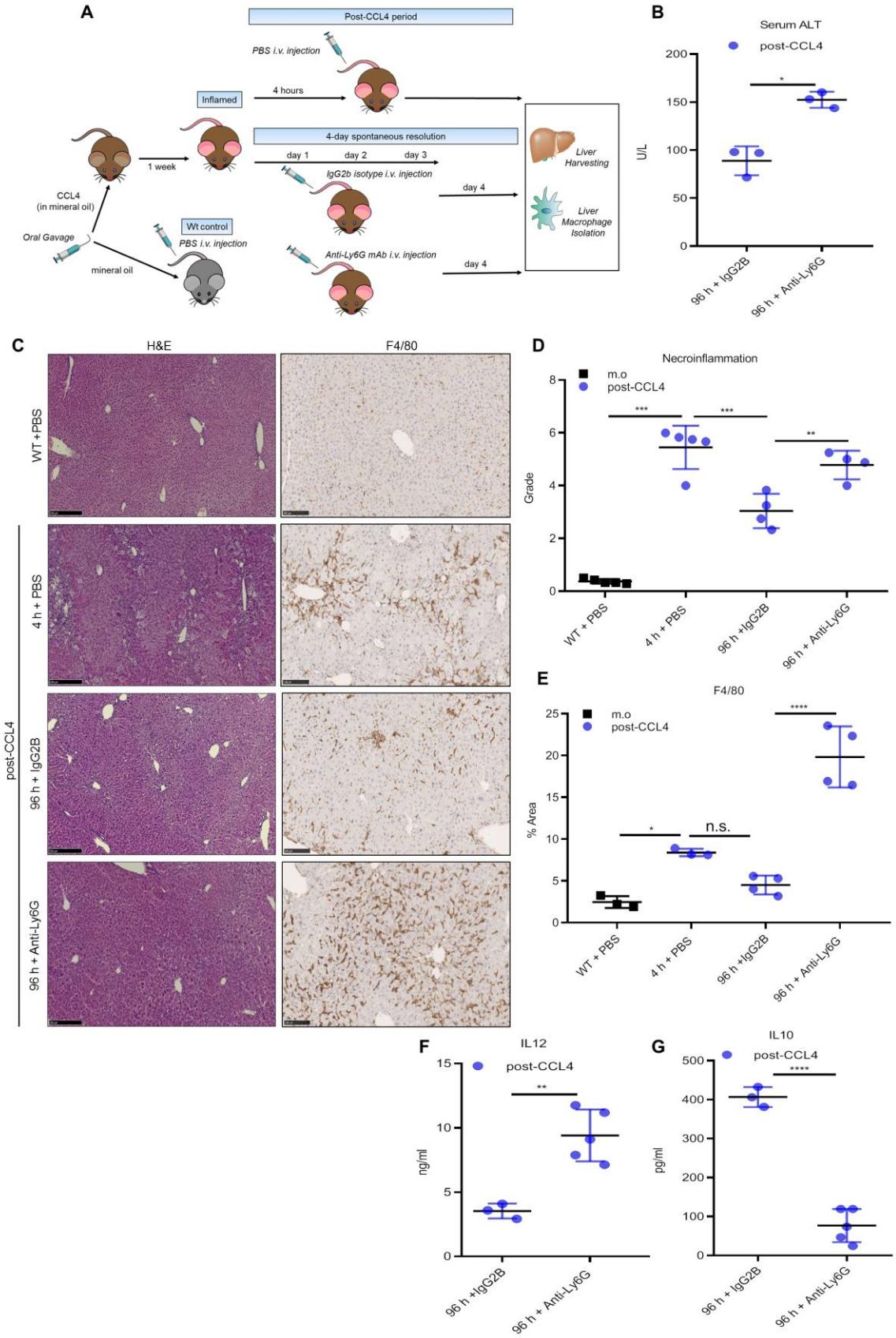
A
Post-CCL4 period
PBS i.v. injection
4 hours
Inflamed
4-day spontaneous resolution
day 1
day 2
day 3
IgG2b isotype i.v. injection
day 4
Anti-Ly6G mAb i.v. injection
day 4
Liver Harvesting
Liver Macrophage Isolation
1 week
CCL4 (in mineral oil)
Oral Gavage
mineral oil
Wt control
PBS i.v. injection
B
Serum ALT
post-CCL4
U/L
96 h + IgG2B
96 h + Anti-Ly6G
C
H&E
F4/80
WT +PBS
4 h + PBS
96 h + IgG2B
96 h + Anti-Ly6G
post-CCL4
D
Necroinflammation
m.o
post-CCL4
Grade
WT + PBS
4 h + PBS
96 h +IgG2B
96 h + Anti-Ly6G
E
F4/80
m.o
post-CCL4
% Area
n.s.
F
IL12
post-CCL4
ng/ml
G
IL10
post-CCL4
pg/ml

Figure 1 Neutrophil depletion impairs spontaneous resolution of liver inflammation (SRLI) (A) Schematic representation of the experimental design of the systemic neutrophil depletion model during SRLI after treatment with CCL4. (**B**) Serum ALT levels measured by colorimetry. **P*<0.05, two-tailed unpaired t-test, n=3/group (**C**) Representative images of liver sections stained for parenchymal and non-parenchymal cells and total macrophages with H&E and antibody to F4/80, respectively. Bars= 100 μm. n=4-5/group (**D**) Grade of necroinflammation as assed following Ishak System. ***P*<0.01; ****P*<0.001, one-way ANOVA, n= 3-6/group (**E**) Percentage of F4/80 positive area in ten randomly selected fields, by computerized image analysis. Not significant (n.s.); **P*<0.05; *****P*<0.0001, one-way ANOVA, n= 3-4/group (**F-G**) Serum levels of IL12 and IL10 quantified by colorimetric and luminescent ELISA, respectively, using biotinylated mouse mAbs for IL12 or IL10. ***P*<0.01; *****P*<0.0001, two-tailed unpaired t-test. Data are represented as means ± SD, n=3-5/group. Representative experiment of two independent repeats.

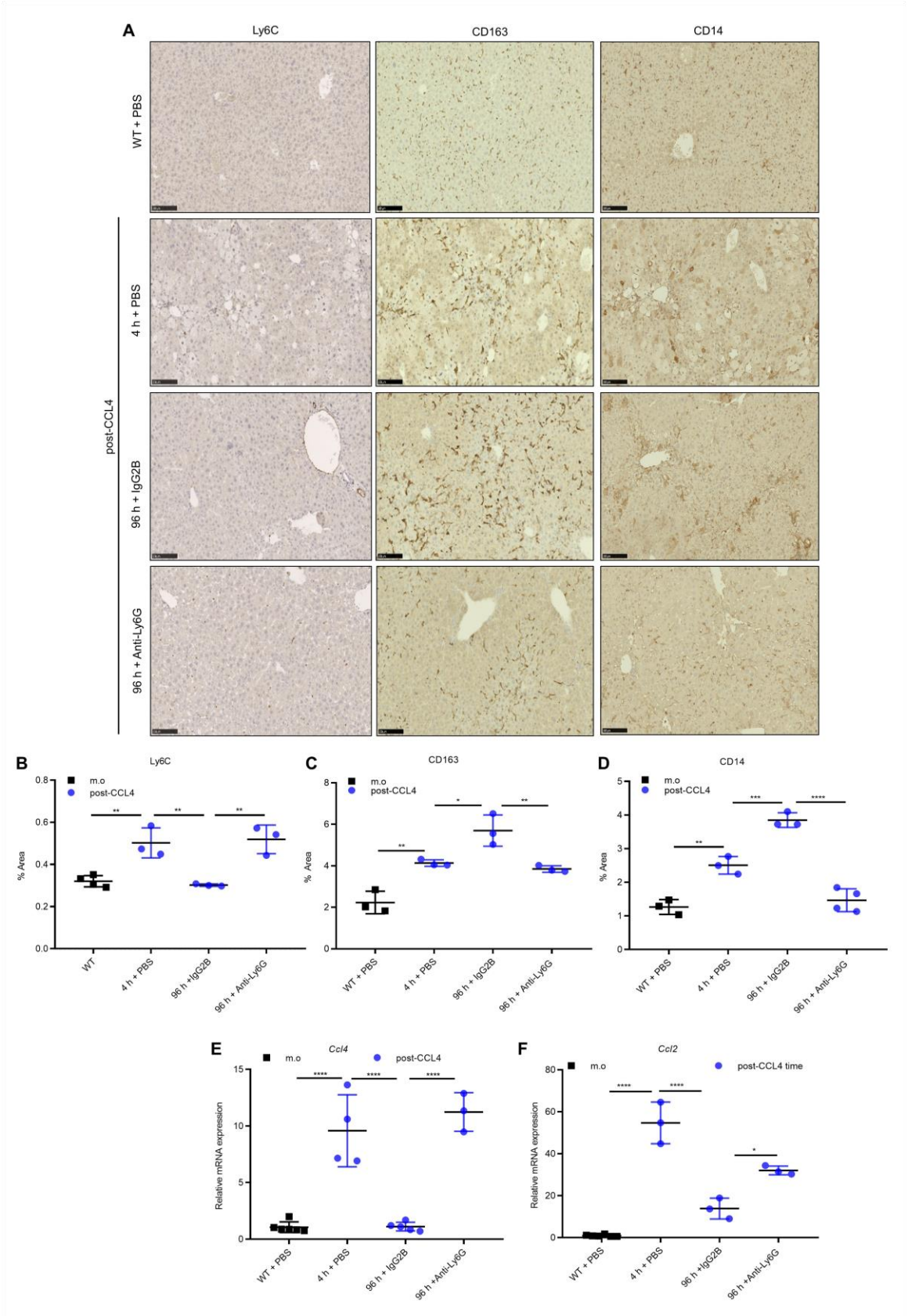
A
Ly6C
CD163
CD14
WT + PBS
post-CCL4
4 h + PBS
96 h + IgG2B
96 h + Anti-Ly6G
B
Ly6C
m.o
post-CCL4
% Area
WT
4 h + PBS
96 h +IgG2B
96 h + Anti-Ly6G
C
CD163
D
CD14
E
Ccl4
Relative mRNA expression
F
Ccl2
post-CCL4 time

Figure 2 Neutrophil depletion results in persistence of classically activated hepatic macrophages during SRLI (A) Representative microphotographs of dissected livers stained for pro-inflammatory, restorative and anti-macrophages using antibodies against Ly6C, CD163 or CD14, respectively. Bars= 100 μm. (**B-D**) Area positive for Ly6C, CD163 or CD14 expressed as percentage and assessed with Image J software in 10 aleatory selected images. **P*<0.05; ***P*<0.01; ****P*<0.001*;* *****P*<0.0001, one-way ANOVA, n= 3-4/group (**E-F**) Hepatic expression of *Ccl4* and *Ccl2* transcripts as measured by qRT-PCR, relative to *B2m* mRNA housekeeping gene. **P*<0.05; *****P*<0.0001, one-way ANOVA**.** Data are represented as means ± SD, n=3-6/group. Representative experiment of two independent repeats.

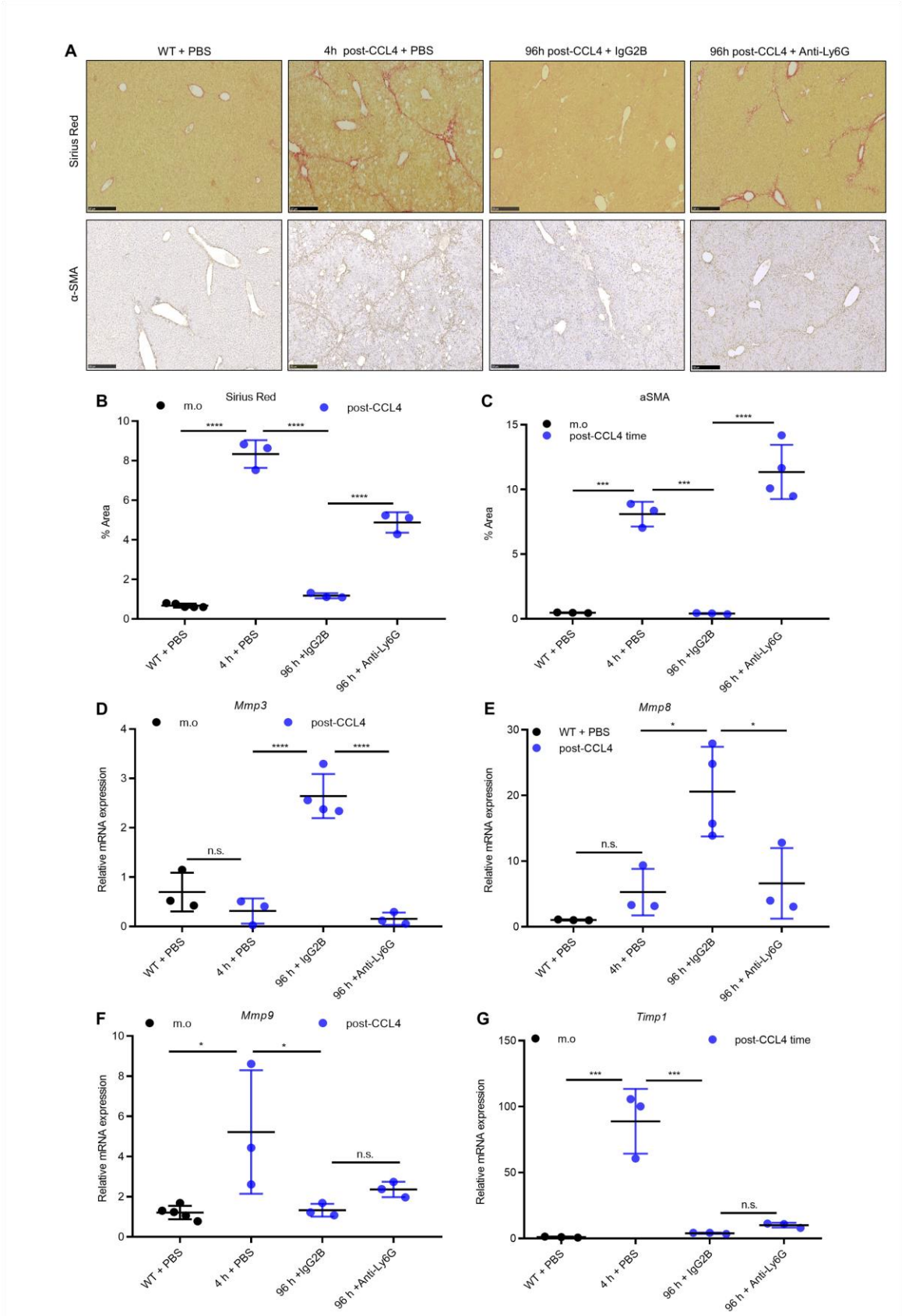
A
WT + PBS
4h post-CCL4 + PBS
96h post-CCL4 + IgG2B
96h post-CCL4 + Anti-Ly6G
Sirius Red
α-SMA
B
Sirius Red
m.o
post-CCL4
% Area
WT + PBS
4 h + PBS
96 h +IgG2B
96 h + Anti-Ly6G
C
aSMA
m.o
post-CCL4 time
% Area
D
Mmp3
Relative mRNA expression
n.s.
E
Mmp8
WT + PBS
post-CCL4
F
Mmp9
G
Timp1
post-CCL4 time

Figure 3 Neutrophil deletion aggravates spontaneous resolution of early liver fibrosis

(A) Sections from livers of experiment in **Figure 1 A** displaying representative staining for collagen and for a subset of activated HSCs with Sirius Red or anti-αSMA mAb, respectively. Scale bars=100 m. (**B-C**) Area of Sirius Red and α-SMA expressed as percentages of 10 aleatory selected microscopic fields, quantified by Image J. ****P*<0.001; *****P*<0.0001, one-way ANOVA, n= 3-6/group (**D-G**) Relative mRNA expression of *Mmp3*, *Mmp8, Mmp9* and *Timp1* genes from liver homogenates of experiment in **Figure 1 A**, assessed by real time RT-PCR and normalized to *B2m* mRNA housekeeping gene. Not significant (n.s.); **P*<0.05; ***P*<0.01; ****P*<0.001; *****P*<0.0001, one-way ANOVA, n= 3-6/group. Data are shown as means ± SD. Representative experiment of two independent repeats.

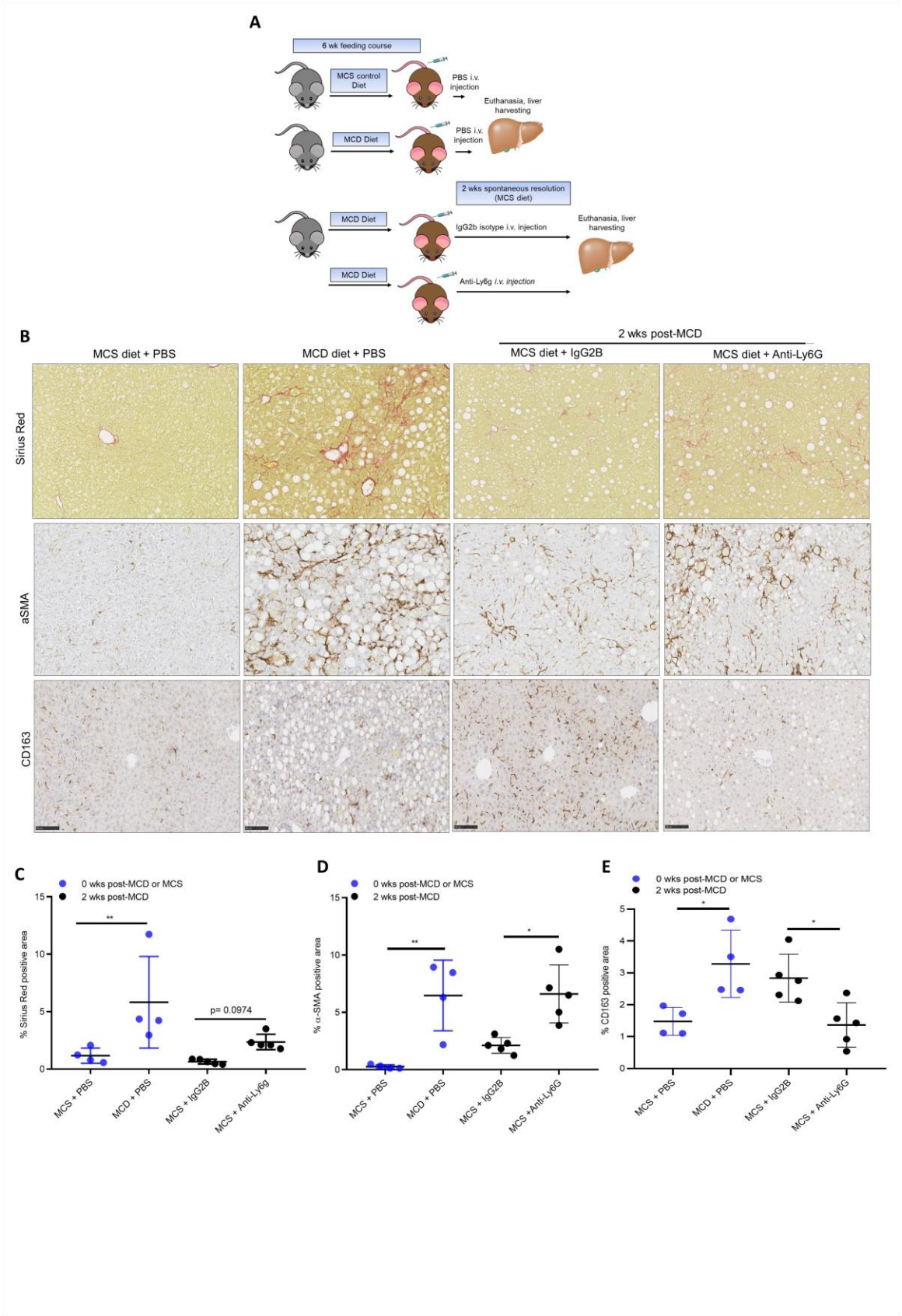
A
6 wk feeding course
MCS control Diet
PBS i.v. injection
Euthanasia, liver harvesting
MCD Diet
PBS i.v. injection
2 wks spontaneous resolution (MCS diet)
MCD Diet
IgG2b isotype i.v. injection
Euthanasia, liver harvesting
MCD Diet
Anti-Ly6g i.v. injection
B
2 wks post-MCD
MCS diet + PBS
MCD diet + PBS
MCS diet + IgG2B
MCS diet + Anti-Ly6G
Sirius Red
aSMA
CD163
C
0 wks post-MCD or MCS
2 wks post-MCD
% Sirius Red positive area
p= 0.0974
MCS + PBS
MCD + PBS
MCS + IgG2B
MCS + Anti-Ly6g
D
0 wks post-MCD or MCS
2 wks post-MCD
% α-SMA positive area
MCS + PBS
MCD + PBS
MCS + IgG2B
MCS +Anti-Ly6G
E
0 wks post-MCD or MCS
2 wks post-MCD
% CD163 positive area
MCS + PBS
MCD + PBS
MCS + IgG2B
MCS + Anti-Ly6G

Figure 4 Neutrophil abrogation impairs the spontaneous resolution of inflammation and advanced fibrosis in NASH (A) Experimental design showing neutrophil depletion with anti-Ly6G or control IgG2B mAb during two weeks (spontaneous resolution period) after a 6-week course feeding with control MCS or MCD diet to induce fibrotic NASH; mice treated with PBS were euthanized immediately after feeding with MCD or MCS diet to serve as the inflamed or Wt controls, respectively. (**B**) Representative immunohistochemical images of accumulated collagen, activated HSCs and anti-inflammatory macrophages stained with Sirius Red or antibodies for αSMA or CD163, respectively. Scale bars= 100 μm (**C-E**) Percentage of area positive for Sirius Red, αSMA or CD163 calculated in 10 aleatory selected images; p= 0.0974, *p<0.05, **p<0.01, one-way ANOVA, n=4-5. Data are shown as means ± SD. Representative experiment of two independent repeats.

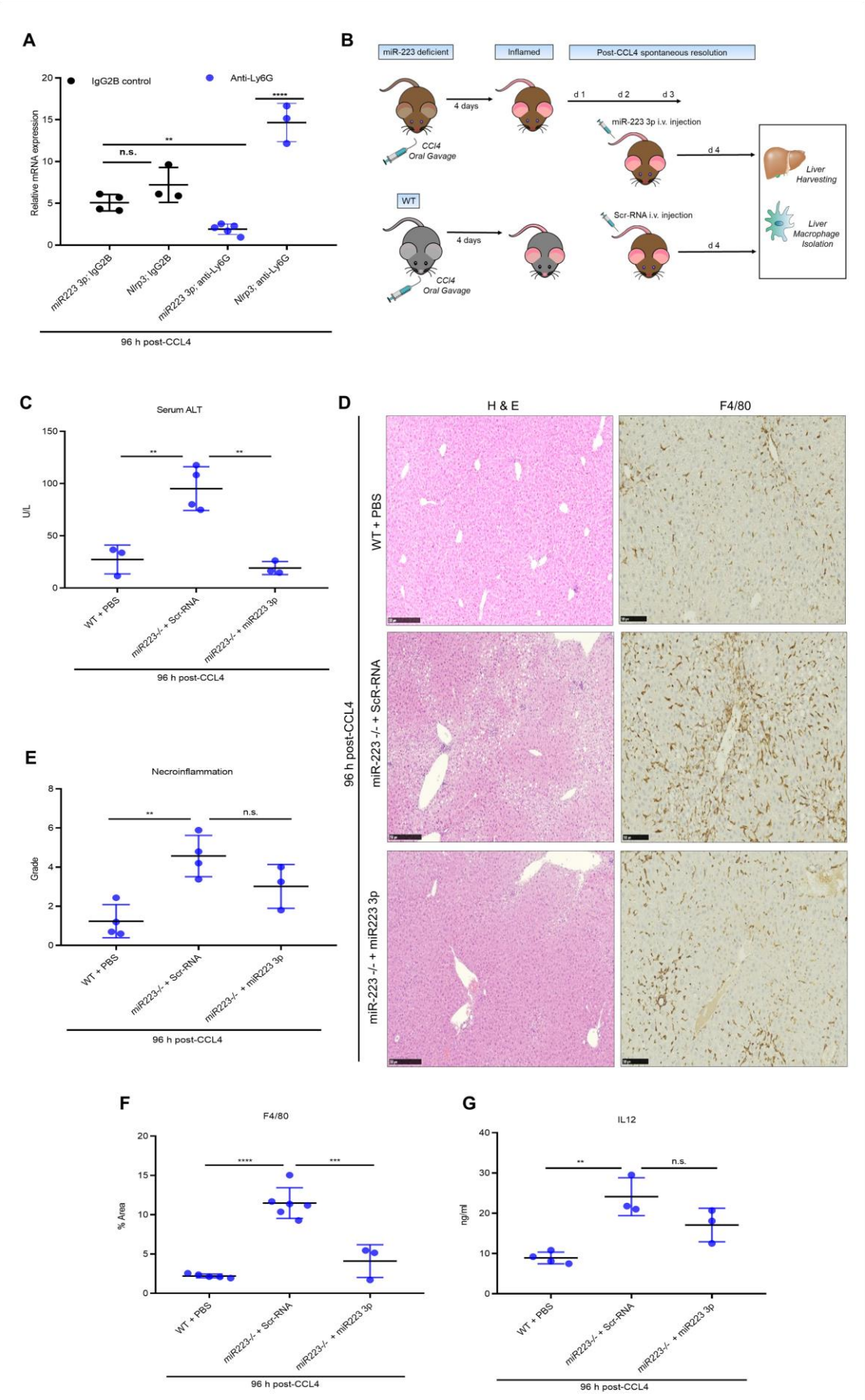
A
IgG2B control
Anti-Ly6G
Relative miRNA expression
n.s.
**
****
miR223 3p; IgG2B
Nlrp3; IgG2B
miR223 3p; anti-Ly6G
Nlrp3; anti-Ly6G
96 h post-CCL4
B
miR-223 deficient
Inflamed
Post-CCL4 spontaneous resolution
4 days
d 1
d 2
d 3
miR-223 3p i.v. injection
d 4
CCl4
Oral Gavage
Liver
Harvesting
WT
Scr-RNA i.v. injection
Liver
Macrophage
Isolation
C
Serum ALT
U/L
WT + PBS
miR223-/- + Scr-RNA
miR223-/- + miR223 3p
96 h post-CCL4
D
H & E
F4/80
WT + PBS
miR-223 -/- + ScR-RNA
miR-223 -/- + miR223 3p
96 h post-CCL4
E
Necroinflammation
Grade
F
F4/80
% Area
G
IL12
ng/ml

Figure 5 Regulation of SRLI by miR-223 (A) Expression of miR-223 3p and *Nlrp3* transcripts in isolated macrophages from livers of experiment in **Figure 1 A** assessed by real time RT-PCR and normalized to *U6* or *B2m* housekeeping genes, respectively. Not significant (n.s.);***P*<0.01; *****P*<0.0001, two-way ANOVA, n=3-5/group. (**B**) Experimental design of the miR-223 post-transcriptional replacement model during spontaneous recovery of liver inflammation after CCL4 treatment. (**C**) Levels of serum ALT in serum as measured by colorimetry. **P*<0.01, one-way ANOVA, n= 3-4/group (**D**) Liver sections representing images of liver cells and total macrophages after staining with H&E and anti-F4/80 antibody, respectively. Scale bars= 100 μm. (**E**) Necroinflammatory grade examined according to the Ishak System. Not significant (n.s.); ***P*<0.01, one-way ANOVA, n=3-4/group (**F**) Percentage of area positive for F4/80 in ten randomly chosen images quantified by Image J. Not significant (n.s.); ****P*<0.001; *****P*<0.0001, one-way ANOVA, n= 3-6/group (**G**) Serum levels of IL12 measured by colorimetric ELISA. Not significant (n.s.); ***P*<0.01, two-tailed unpaired t-test, n= 3-4/group Data are shown as means ± SD.

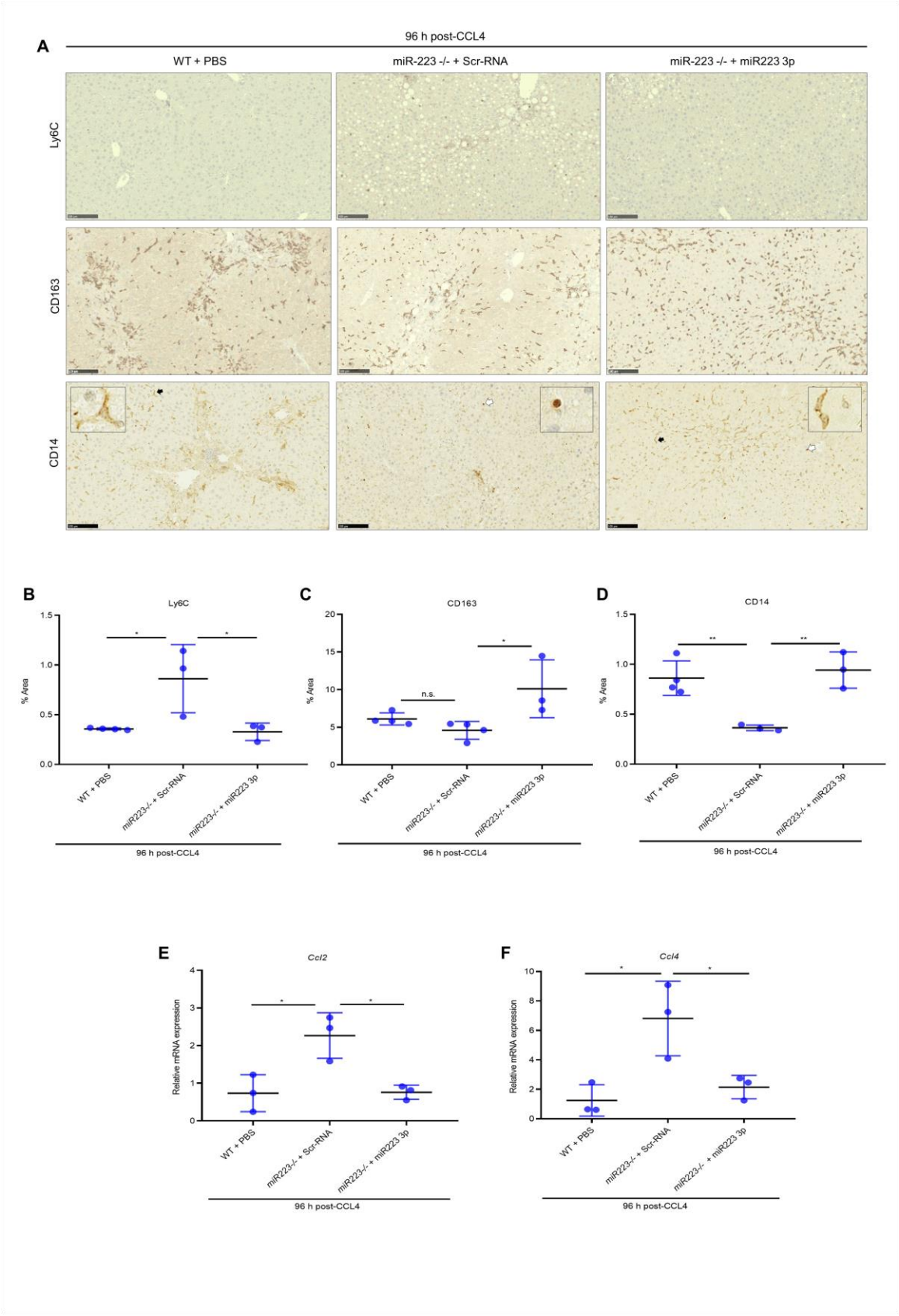
A
96 h post-CCL4
WT + PBS
miR-223 -/- + Scr-RNA
miR-223 -/- + miR223 3p
Ly6C
CD163
CD14
B
Ly6C
% Area
C
CD163
n.s.
D
CD14
WT + PBS
miR223-/- + Scr-RNA
miR223-/- + miR223 3p
96 h post-CCL4
E
Ccl2
Relative mRNA expression
F
Ccl4

Figure 6 *miR-223* deficiency reduces the hepatic restorative macrophage compartment in SRLI (A) Representative pictures of liver sections exhibiting pro-inflammatory, restorative and anti-inflammatory macrophages as stained with anti-Ly6C, CD163 or CD14, respectively. Scale bars= 100 m. (**B-D**) Percentage of area positive for Ly6C, CD163 and CD14 in ten randomly chosen images quantified by Image J. Not significant (n.s.); **P*<0.05; ***P*<0.01; ****P*<0.001; *****P*<0.0001, one-way ANOVA, n=3-4/group (**F-G**) *Ccl2* and *Ccl4* mRNA expression normalized to *B2m* mRNA and measured by real time RT-PCR. **P*<0.05, one way-ANOVA, n= 3/group. Data are shown as means ± SD.

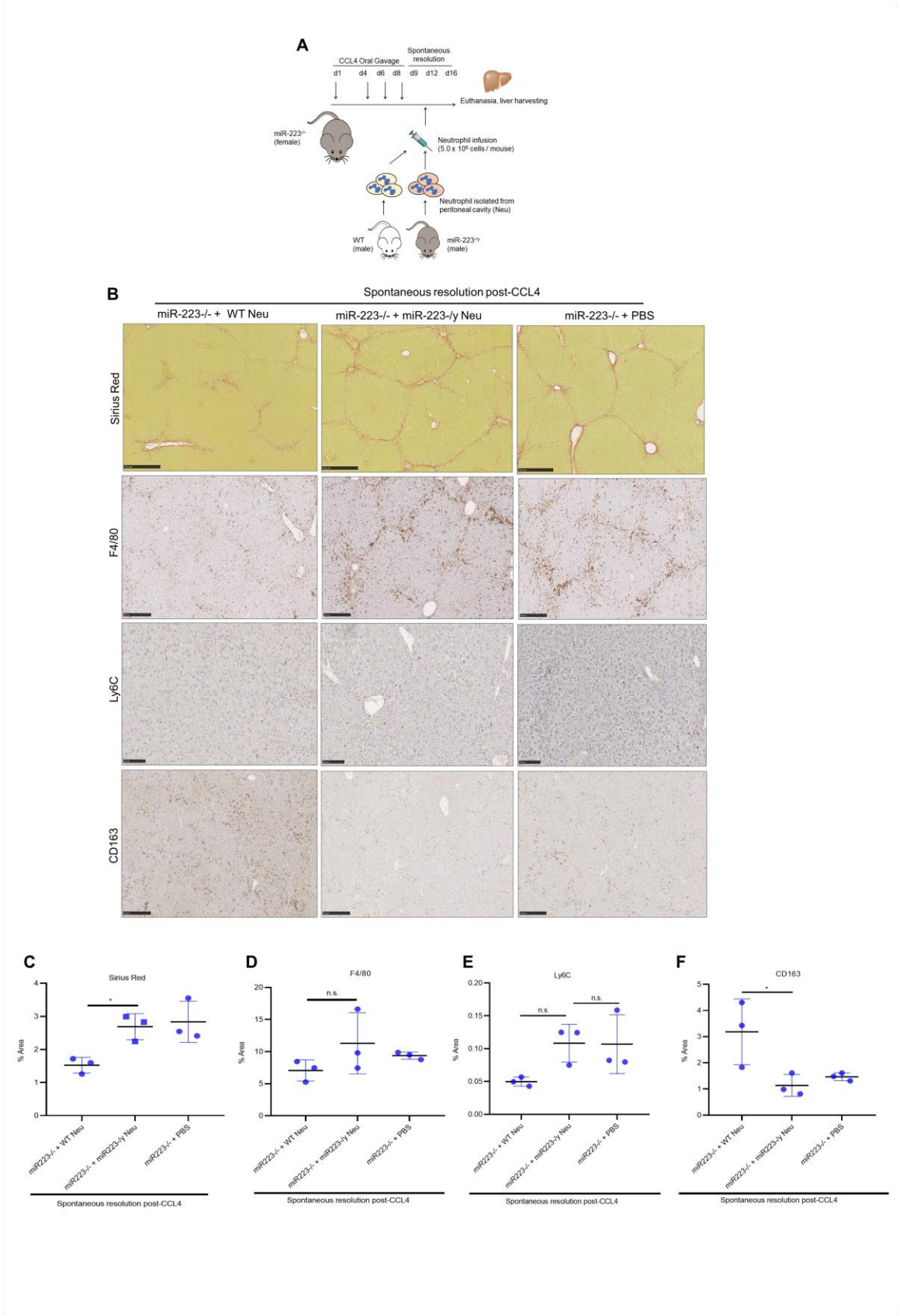
A
CCL4 Oral Gavage
Spontaneous resolution
d1 d4 d6 d8 d9 d12 d16
Euthanasia, liver harvesting
miR-223-/- (female)
Neutrophil infusion (5.0 x 10⁶ cells / mouse)
Neutrophil isolated from peritoneal cavity (Neu)
WT (male)
miR-223-/y (male)
B
Spontaneous resolution post-CCL4
miR-223-/- + WT Neu
miR-223-/- + miR-223-/y Neu
miR-223-/- + PBS
Sirius Red
F4/80
Ly6C
CD163
C
Sirius Red
% Area
D
F4/80
n.s.
E
Ly6C
n.s.
F
CD163
*
miR223-/- + WT Neu
miR223-/- + miR223-/y Neu
miR223-/- + PBS
Spontaneous resolution post-CCL4

Figure 7 Neutrophils accelerate the spontaneous resolution of inflammation and fibrosis in miR-223 deficient mice (A) Experimental design of Wt or miR-223-/- neutrophils infusion to miR-223-/- mice during SRLI after a-week course of CCL4 gavage. (**B**) Representative micrographs of collagen accumulation, total macrophages and monocytes stained with Sirius Red or F4/80, Ly6C or CD163 antibody, respectively. Scale bars= 100 µm. (**C-F**) Percentage of area positive for Sirius Red, F4/80, Ly6C or CD163 analysed in 10 independent images. *P<0.05, two-way ANOVA, n=3. Results are displayed as means ± SD. Representative experiment of two independent repeats.

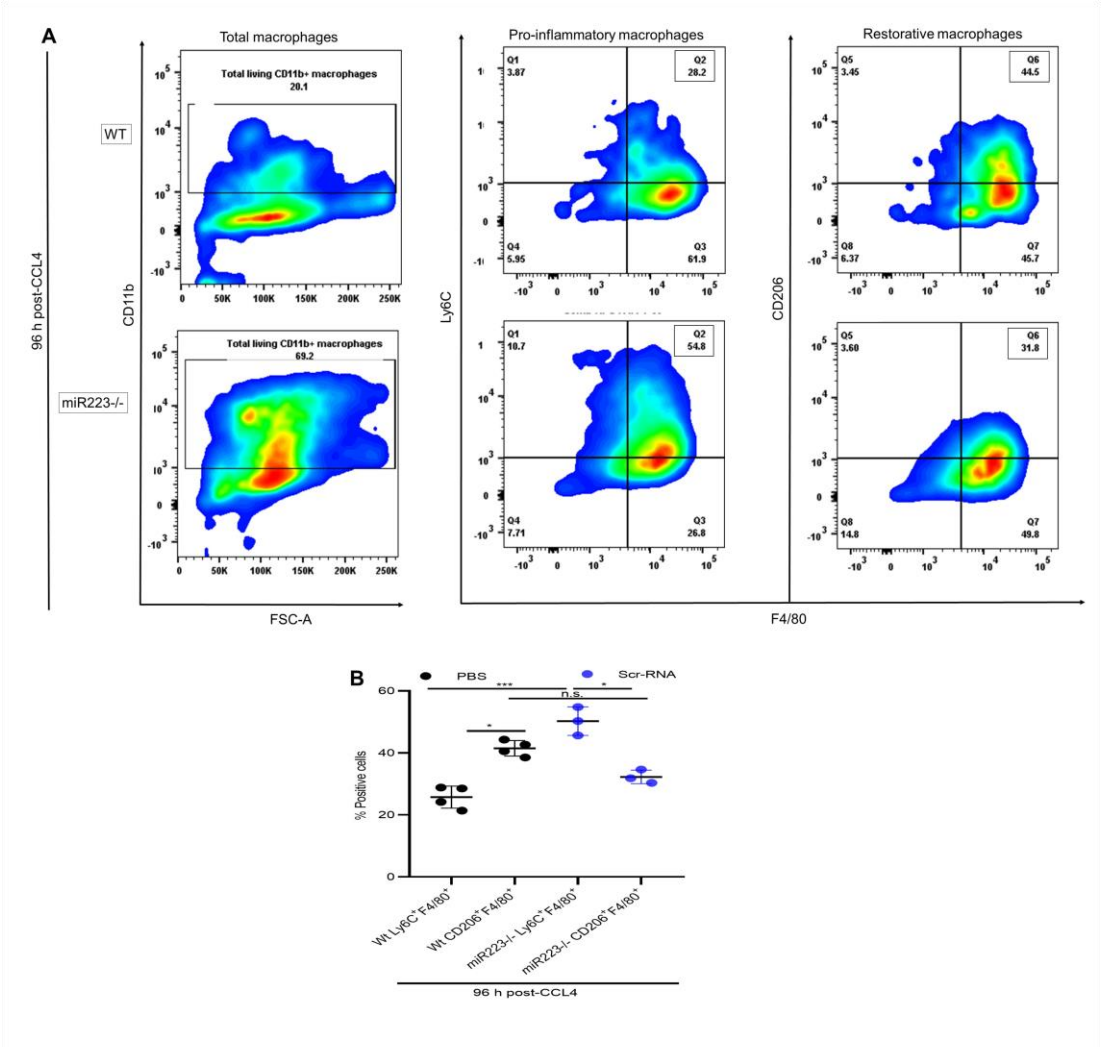

Figure 8 Deletion of miR-223 impairs alternative activation of hepatic macrophages in SRLI (A) Representative FACS analysis of primary hepatic macrophages from mice of experiment in **Figure 4b** showing single CD11b (total macrophages) and double Ly6C and F4/80 (pro-inflammatory macrophages) or CD206 and F4/80 (restorative macrophages) positive cells. Upper quadrants on the CD11B axis and upper right quadrant on the Ly6C and F4/80 or CD206 and F4/80 axis represents the percentage of single positive or double positive cells, respectively. (**b**) Percentage of double positive Ly6C and F4/80 or CD206 and F4/80 cells. Not significant (n.s.); **P*<0.05; ****P*<0.001, two-way ANOVA, n= 3-4. Results are displayed as means ± SD. Representative experiment of two repeats.

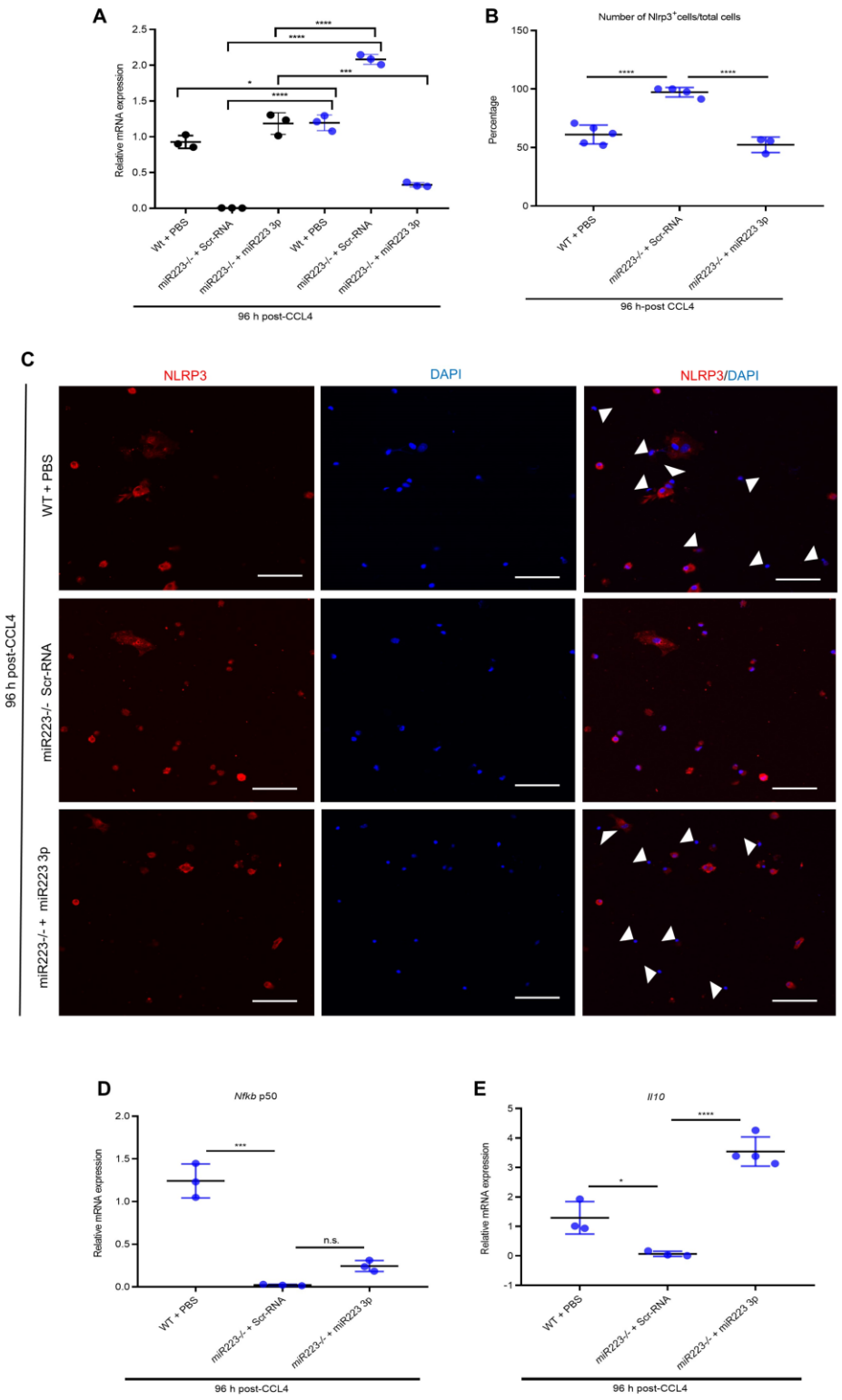
A
Relative mRNA expression
Wt + PBS
miR223-/- + Scr-RNA
miR223-/- + miR223 3p
96 h post-CCL4
B
Number of Nlrp3+cells/total cells
Percentage
96 h post-CCL4
C
NLRP3
DAPI
NLRP3/DAPI
WT + PBS
miR223-/- Scr-RNA
miR223-/- + miR223 3p
96 h post-CCL4
D
Nfkb p50
n.s.
E
Il10

Figure 9 miR-223 abolition augments NLRP3 expression in hepatic macrophages during SRLI. Macrophages were isolated from mice livers of experiment in **Figure 5 B** (**A**) Expression of miR-223 3p and *Nlrp3* transcripts normalized by *B2m* mRNA and measured by real time qRT-PCR. *P<0.05; ***P<0.001; ****P<0.0001, two-way ANOVA, n= 3 (**B**) Number of cells positive for anti-NLRP3 mAb normalized by total cell number per field in 10 random pictures quantified with Image J and expressed as percentage. ****P<0.0001, one-way ANOVA, n= 3-5/group **(C)** Representative confocal immunofluorescent images of NLRP3-expressing cells (red) and nuclei (blue) stained with anti-NLRP3 mAb or DAPI, respectively. Individual merges are shown where indicated. For clear distinction of area positive for anti-NLRP3 mAb, white arrows indicate cells and cellular areas negative for anti-NLRP3 mAb. Scale bars= 100 m. (**D-E**) Expression of *NfKb p50* and *Il10* mRNA normalized by *B2m* housekeeping gene and quantified by quantitative RT-PCR. Not significant (n.s.); *P<0.05; ***P<0.001; ****P<0.0001, one-way ANOVA, n= 3-4/group. Data are shown as means ± SD.

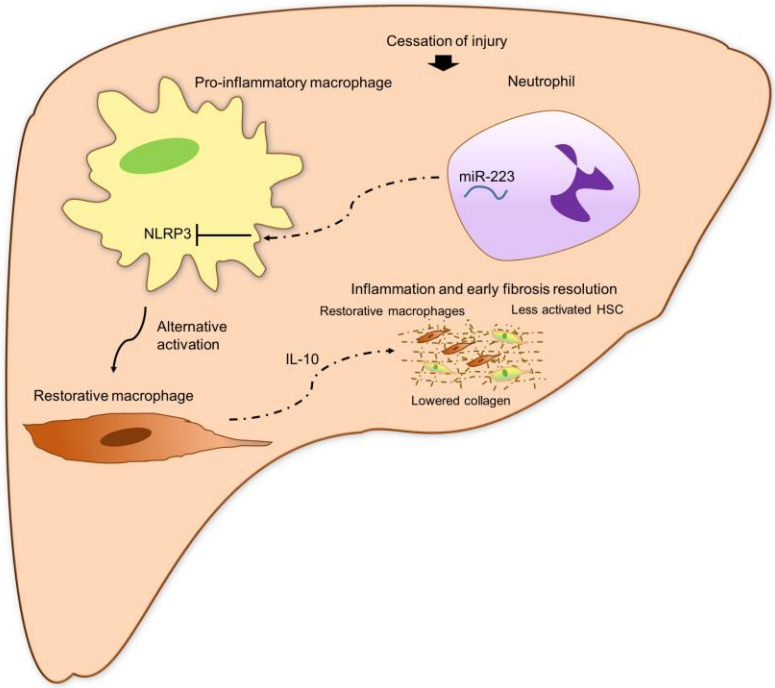

Figure 10 Schematic representation of the potential resolutive mechanism of neutrophils during SRLI. In the liver, neutrophils mediate the silencing of NLRP3 in pro-inflammatory macrophages via miR-223 and induce their alternative activation into a restorative phenotype after the cessation of injury. Then, restorative macrophages release IL10 that indirectly resolves inflammation and early fibrosis by reducing the activation of HSCs and ameliorating *de novo* collagen formation